AUTOMATIC CTR MEASUREMENT FROM CHEST RADIOGRAPH

Mr. Wasin Poncheewin

A Thesis Submitted in Partial Fulfillment of the Requirements
for the Degree of Master of Science Program in Computer Science and Information Technology

Department of Mathematics and Computer Science
Faculty of Science
Chulalongkorn University

Academic Year 2014

การวัดซีทีอาร์แบบอัตโนมัติจากภาพรังสีทรวงอก

นายวศิน ผลชีวิน

วิทยานิพนธ์นี้เป็นส่วนหนึ่งของการศึกษาตามหลักสูตรปริญญาวิทยาศาสตรมหาบัณฑิต
สาขาวิชาวิทยาการคอมพิวเตอร์และเทคโนโลยีสารสนเทศ ภาควิชาคณิตศาสตร์และวิทยาการคอมพิวเตอร์
คณะวิทยาศาสตร์ จุฬาลงกรณ์มหาวิทยาลัย
ปีการศึกษา 2557

Thesis Title	AUTOMATIC CTR MEASUREMENT FROM CHEST RADIOGRAPH
By	Mr. Wasin Poncheewin
Field of Study	Computer Science and Information Technology
Thesis Advisor	Assistant Professor Rajalida Lipikorn, Ph.D.

Accepted by the Faculty of Science, Chulalongkorn University in Partial Fulfillment of the Requirements for the Master's Degree

....Dean of the Faculty of Science

(Professor Supot Hannongbua, Dr.rer.nat.)

THESIS COMMITTEE

....Chairman

(Assistant Professor Nagul Cooharojananone, Ph.D.)

....Thesis Advisor

(Assistant Professor Rajalida Lipikorn, Ph.D.)

....External Examiner

(Suriya Natsupakpong, Ph.D.)

วศิน ผลชีวิน : การวัดซีทีอาร์แบบอัตโนมัติจากภาพรังสีทรวงอก (AUTOMATIC CTR MEASUREMENT FROM CHEST RADIOGRAPH) อ.ที่ปรึกษาวิทยานิพนธ์หลัก: ผศ. ดร. รัชลิดา ลิปิกรณ์, 61 หน้า.

งานวิจัยนี้นำเสนอวิธีการวัดซีทีอาร์แบบอัตโนมัติจากภาพรังสีทรวงอก ด้วยวิธีการประมาณค่าแบบกำลังสองน้อยที่สุดและค่าน้อยสุดสัมพัทธ์ โดยกระบวนการที่นำเสนอนี้แบ่งออกเป็นขั้นตอนต่างๆ เริ่มจากการหาชุดของจุดเริ่มต้นเพื่อใช้ในการคำนวณ จากนั้นทำการวัดขนาดของหัวใจและช่องอกแล้วทำการคำนวณอัตราส่วนของขนาดของหัวใจต่อช่องอกหรือซีทีอาร์ ซึ่งในขั้นตอนการหาชุดของจุดเริ่มต้นนั้นคือการหาบริเวณของช่องอกทั้งหมดโดยใช้ความรู้เบื้องต้นของโครงสร้างในมนุษย์ทั่วไป จากนั้นใช้วิธีการประมาณค่าแบบกำลังสองน้อยที่สุดและค่าน้อยสุดสัมพัทธ์เพื่อหาขอบของหัวใจ แล้วทำการหาขอบของช่องอกเพื่อทำการคำนวณหาอัตราส่วนของขนาดหัวใจต่อช่องอกหรือซีทีอาร์ต่อไป โดยในการทดลองครั้งนี้ใช้ข้อมูลภาพรังสีทรวงอกจากคนไข้จำนวน 523 คน ผลการทดลองประเมินด้วยวิธีการทดสอบสหสัมพันธ์ระหว่างชุดข้อมูลตัวเลข 2 ชุด ซึ่งเป็นผลที่ได้จากการวัดโดยกระบวนการที่นำเสนอเปรียบเทียบกับการวัดโดยนักรังสีวิทยา จากผลการประเมินแสดงให้เห็นว่าค่าสหสัมพันธ์ของค่าซีทีอาร์มีค่าประมาณ 81%

ภาควิชา	คณิตศาสตร์และวิทยาการคอมพิวเตอร์	ลายมือชื่อนิสิต	....
		ลายมือชื่อ อ.ที่ปรึกษาหลัก	....
สาขาวิชา	วิทยาการคอมพิวเตอร์และเทคโนโลยีสารสนเทศ		
ปีการศึกษา	2557		

5572605423 : MAJOR COMPUTER SCIENCE AND INFORMATION TECHNOLOGY
KEYWORDS: CHEST RADIOGRAPH / CARDIO-THORACIC RATIO / COMPUTER-AIDED DIAGNOSIS

WASIN PONCHEEWIN: AUTOMATIC CTR MEASUREMENT FROM CHEST RADIOGRAPH. ADVISOR: ASST. PROF. RAJALIDA LIPIKORN, Ph.D., 61 pp.

This research presents a method to automatically measure cardio-thoracic ratio (CTR) from a chest radiographic image using non-linear least square approximation and local minimum. The proposed method consists of initial boundary point identification, cardiac diameter measurement, thoracic diameter measurement and cardio-thoracic ratio measurement. First, the initial boundary points used to approximate the region of thoracic cavity are identified using general human anatomy features. Then the non-linear least square approximation and local minimum are used to detect the heart boundary. Finally, the thoracic cage boundary is detected and the cardio-thoracic ratio can be measured. The proposed method is tested on a set of 523 chest radiographs. The experimental results are evaluated using correlation test between two sets of numerical measurement which are measured by our proposed method and by the radiologists. The evaluation reveals that the correlation result on CTR is about 81%.

Department: Mathematics and Computer Science
Field of Study: Computer Science and Information Technology
Academic Year: 2014

Student's Signature ....
Advisor's Signature ....

ACKNOWLEDGEMENTS

I would like to greatly thank Asst. Prof. Rajalida Lipikorn, Ph.D., my research advisor, for her guidance and encouragement which is an absolute impetus toward my study.

I am also honored to have Asst. Prof. Nagul Cooharojananone, Ph.D. and Suriya Natsupakpong, Ph.D. as my research chairman and committee.

Beside my advisor and committee, I would like to express my special thanks to Monravee Tumkosit, MD. and Petcharleeya Suwanpradit from Department of Radiology, Faculty of Medicine, Chulalongkorn University and King Chulalongkorn Memorial Hospital for providing clinical advices and research data.

Additionally, this research is financially supported by Centre of Excellence in Mathematics (CEM), Thailand.

Finally, I would like to thank my family, especially my parents, and friends who always supported me throughout my study.

CONTENTS

Page

Page

LIST OF TABLES

LIST OF FIGURES

CHAPTER I
INTRODUCTION

The main purpose of this chapter is to briefly introduce about this research. It consists of objectives, scope of work, problem formulation and the expected outcome of the experiments.

Radiography is one of the most widely used medical procedures performed to diagnose the insight of human body. Chest radiograph is a useful tool for diagnosing the abnormality that occurs in chest cavity and also a source to obtain the size of the heart which is one of the most important factors used to indicate many heart diseases including enlarged heart or cardiomegaly [1]. In the past, cardio-thoracic ratio (CTR) was manually measured by radiologists. At the present, computer-aided diagnosis (CAD) system has become much more popular. This technology has improved the way to diagnose many diseases by giving many advantages such as accuracy, time consumption reduction and automation [2] but a fully automated cardio-thoracic ratio (CTR) measurement has not yet been able to gain a complete reliability from radiologists.

The aim of this research is to propose a new method that can fully automate the cardio-thoracic ratio (CTR) measurement without the use of training data set which can improve accuracy and efficiency.

1.1 Objectives

1) To detect the heart and boundary of the heart.
2) To automatically display cardio-thoracic ratio (CTR) which is the proportion between the widest part of the heart and the widest part of the thoracic-cage.

1.2 Scope of Work

In this study, the proposed method is constrained as follows:

1) Only Digital Imaging and Communications in Medicine (DICOM) file format is allowed as an input image.
2) Only Posterior-Anterior (PA) radiographs are allowed.

3) Input images must be able to be analyzed by radiologists.
4) Input images must have high contrast.

1.3 Problem Formulation

Although, cardio-thoracic ratio (CTR) measurement is commonly performed in radiograph by a radiologist for a long time but even with today's technologies, an automatic procedure still not yet a common tool to use in diagnosis process due to an unreliable results.

However, the measurement made by a radiologist could possibly result in individual variation and time consuming. Therefore, automatic system with high accuracy rate will be a solution for this problem.

1.4 Expected Outcomes

1) The method that can measure cardio-thoracic ratio (CTR) from chest radiograph automatically.
2) The method that reduces time complexity and man power.
3) The method that increases the accuracy and efficiency of the automated diagnosis.

CHAPTER II

FUNDIMENTAL KNOWLEDGE AND LITERATURE REVIEW

This chapter provides a fundamental knowledge about the technique used in the proposed method and also describes related work in the literature review section to give better understanding about this work.

2.1 Fundamental Knowledge

2.1.1 Digital Imaging and Communication in Medicine (DICOM)

DICOM is a standard format for handling, storing, printing and transmitting information in a medical image. It contains all the information about a patient within the file such as name, ID, age and etc. which are called attributes.

2.1.2 Histogram Equalization

This method enhances the contrast of an image by transforming intensity values of an image so that the histogram of the output image is distributed evenly as shown in Figure 1.

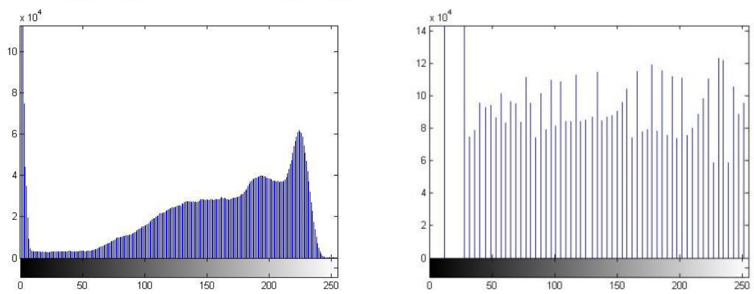

Figure 1 Histogram equalization

2.1.3 Median Filtering

This filtering technique is used to remove noise from an image. It is performed on an image by ranking the intensities of all pixels in an $m\ x\ n$ neighbor and replacing the center pixel's intensities with the median intensity.

For example:

Using 3x3 filter

4	3	5
3	10	5
4	2	5

Figure 2 Original intensities within median filter.

The original intensities in the neighbor under the filter are as shown in Figure 2 and it's ranked in ascending order as 2, 3, 3, 4, 4, 5, 5, 5, 10.

The median value within the filter is 4 thus the value of the center pixel in the filter will be changed to 4 as shown in Figure 3:

4	3	5
3	**4**	5
4	2	5

Figure 3 Modified intensity with median filter.

2.1.4 Density-Based Spatial Clustering of Application with Noise (DBSCAN)

DBSCAN is a data clustering algorithm [3]. It is based on the concept of density-reachability. It is an idea of whether point B can be directly searched from point A under the condition that it is not within a given distance. Figure 4 shows that points B and C are density-reachable by point A, which is a core point, and thus they are density-connected and belong to the same cluster while point N is not reachable, therefore, it will be defined as noise.

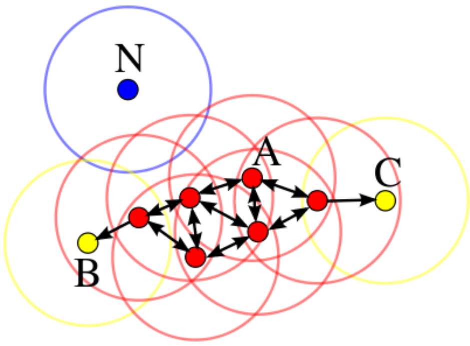

Figure 4 DBSCAN

http://en.wikipedia.org/wiki/DBSCAN

Data is separated into groups by using the minimum distance between each points and the minimum number of points required to form a dense region as parameters.

2.1.5 Polynomial Curve Fitting

Curve fitting is used to find the best fit curve from a given dataset. In this work, polynomial curve fitting is used to estimate the boundary on both sides of the heart from the given dataset consisting of points which are retrieved from the gradient procedure. Examples of polynomial curve fitting of 2nd degree and 4th degree are shown in Figure 5.

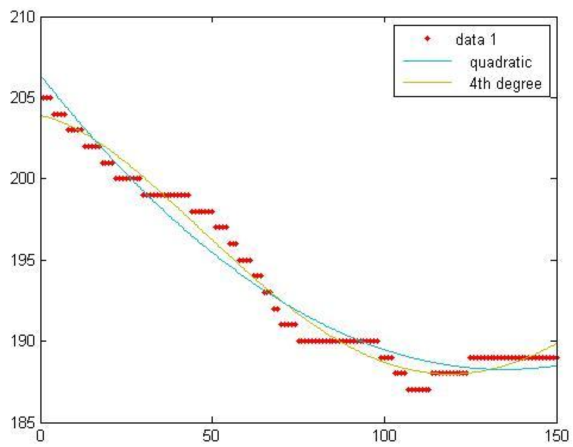

Figure 5 Example of polynomial curve fitting

The curve of the estimate line is based on the degree used in the polynomial equation as follows:

Let $f(x,y)$ represent an input image where (x,y) are the coordinates of each pixel and $f(x)$ be an intensity of any pixel from each column of an image. The polynomial equation is written as:

$$f(x) = c_1x^n + c_2x^{n-1} + \cdots + c_nx + c_{n+1} \qquad (1)$$

where n is the degree of the polynomial equation and c_j is the coefficient value of the polynomial which can be calculated from

$$\sum_{k=1}^{n+1}\left(\sum_{i=1}^{M} x_i^{2n+2-j-k}\right)c_j = \sum_{i=1}^{M} x_i^{j} f(x_i) \qquad (2)$$

Deviation of the intensity curve from each data point is

$$e_i = f(x_i) - p(x_i), i = 1, \dots, M \qquad (3)$$

where M is the number of pixels in each column. By using least square error, $\frac{\partial E}{\partial c_j} = 0, j = 1, \dots, n+1$ such that E is the sum of the squared deviation:

$$E = \sum_{i=1}^{M} e_i^2$$

2.1.6 Pearson's Linear Correlation Coefficient

Pearson's correlation coefficient is a measure of the linear correlation between two variables X and Y, giving a value between +1 and -1, where 1 is a positive correlation, 0 is no correlation, and -1 is a negative correlation as shown in Figure 6.

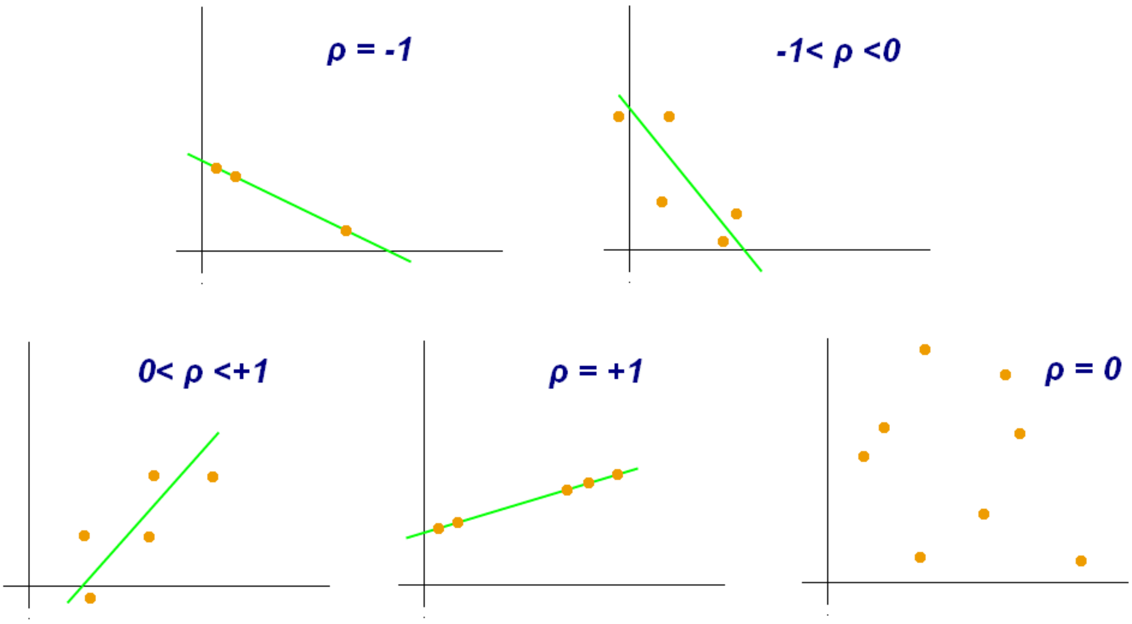

Figure 6 Pearson's linear correlation coefficient

The formula is

$$p(x,y) = \frac{\sum(x-\bar{x})(y-\bar{y})}{\sqrt{\sum(x-\bar{x})^2(y-\bar{y})^2}}$$

where $p(x,y)$ is a correlation result, $\bar{x}$ and $\bar{y}$ are the sample means of x in dataset 1 and y in dataset 2, respectively .

2.2 Literature Review

Various techniques to create a computer-aided diagnosis (CAD) in chest radiograph have been proposed. Related work about cardiomegaly detection and cardio-thoracic ratio (CTR) measurement is the main focus. The study by M. Ilovar and L. Šajn uses average intensity and image blurring for image initiation then uses edge detection to locate the position of the heart. After finding the widest part of the heart, the horizontal line is drawn outward from the heart boundary to each boundary of the image and identify the widest part of the thoracic cage by locating the brightest intensity from each side of the body [4]. However, this method of measuring the CTR is not precise according to the actual definition by Danzer, C.S. [5]. Ha Dai Duong and Dao Thanh had developed a segmentation algorithm using texture-based results in a rough estimation of three areas: dark region, gray region and light region which are not yet suitable for cardio-thoracic ration (CTR) measurement due to precision matters [6]. Ishida and his colleagues developed an algorithm that uses histogram analysis and edge detection technique with feature analysis to diagnose the cardiomegaly but the region of interest (ROI) which is used in histogram analysis is manually selected [7]. Another excellent work has been proposed by Samuel G. Armato III and his colleagues which uses iterative global and local histogram analysis to determine the proper threshold value used for the chest radiograph but the region of interest (ROI) which is used in histogram analysis is also manually selected and the evaluation method was unreliable due to radiologist ranking [8]. Another novel method was developed by Sezaki Nobuhiko and Ukena Kohji which can compute the cardio-thoracic ratio (CTR) with good results and complexity but it must be installed on their special instrument [9]. Beside all of the technical work, there are a survey and a comparative study of other proposed methods that provide useful information [10, 11]. The survey gives information about existing techniques that have been used in computer-aided diagnosis (CAD) in chest radiograph. The content was separated into three sections: enhancement, segmentation (e.g. lung fields, rib cage) and analysis (e.g. size measurement, lung nodule detection, texture analysis) [10]. A comparative study in segmentation focused on three methodologies: active shape models (ASM), active appearance models (APM) and pixel classification (PC). These methodologies need training data in order to create a landmark and an initial model used within algorithms. It surely yields a good result in segmentation but not better than other algorithms without a model or training data. Therefore, those methodologies are not appropriate candidates for this work [11].

CHAPTER III

PROPOSED METHODOLOGY

The proposed methodology uses non-linear least square approximation and local minimum to measure cardio-thoracic ratio (CTR) automatically from chest radiograph. It consists of the following steps (as shown in Figure 7):

1) Perform image pre-processing.
2) Identify Initial boundary points.
3) Measure cardiac and thoracic diameters.
4) Calculate the cardio-thoracic ratio (CTR).

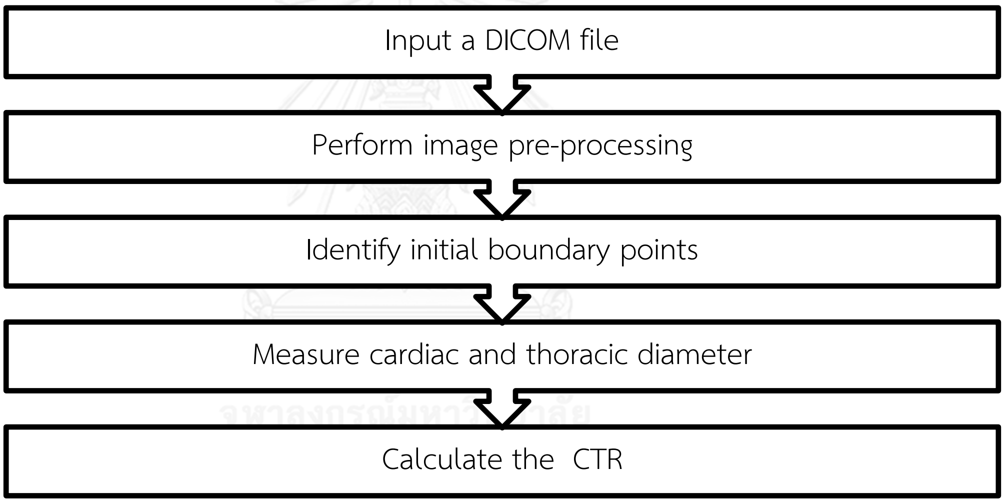

Figure 7 Work process of the proposed methodology

3.1 Image Pre-processing

The original DICOM files, obtained from an X-Ray machine with all constraints as mentioned in the scopes of work, are used as input images. Each image is resized and converted to JPEG file format. The visibility of the organs in each image is enhanced by using histogram equalization and median filter. Then, the average intensity of the processed image is calculated and used as threshold value to convert the original gray scale image to a binary image as shown in Figures 8, 9, 10 and 11.

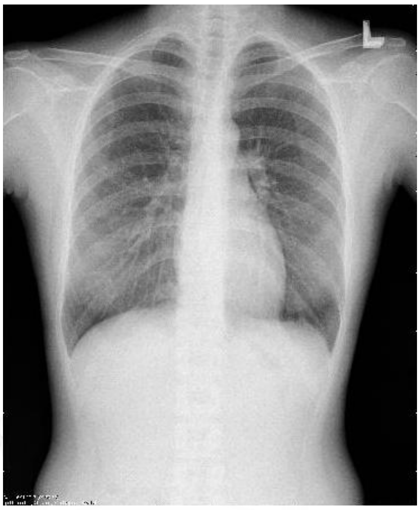

Figure 8 Original DICOM file

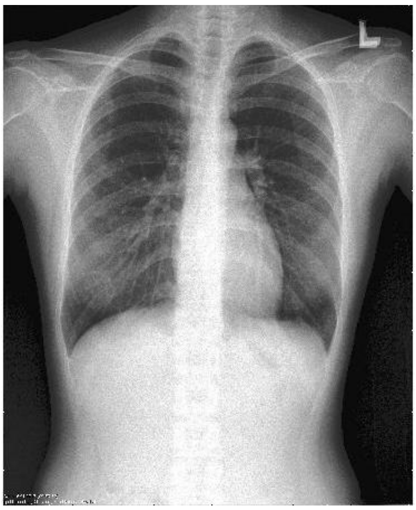

Figure 9 Using histogram equalization

Figure 10 Using median filter

Figure 11 Binary image

3.2 Initial Boundary Point Identification

In this step, the initial region of lung is identified by:

1) Identify the initial center point of the body.
2) Identify the initial left and right boundary points of the lung.
3) Identify the initial upper and lower boundary points of the lung.

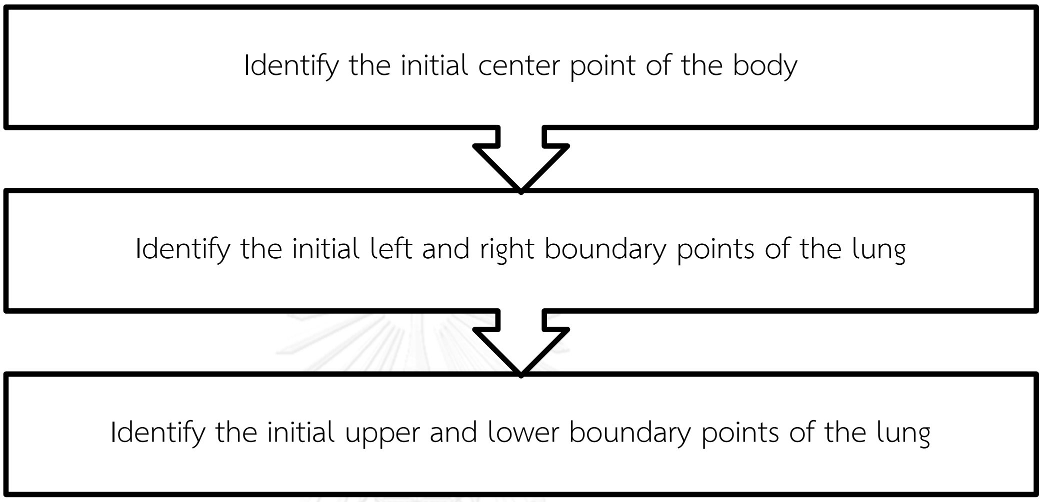

Figure 12 Initial boundary point identification process

3.2.1 The Initial Center Point of the Body Identification

This point is identified by setting the x-coordinate to equal to the middle column of the white region on the last row of a binary image obtained from the previous step of each patient which is assumed to represent the patient's body and setting the y-coordinate to be half of the height of an image as shown in Figure 13. This point is shown as '*' in Figure 17.

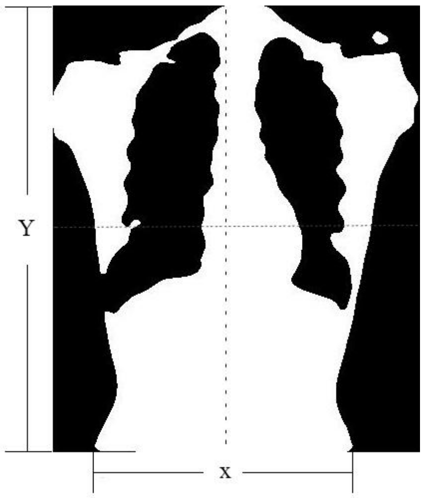

Figure 13 Initial center point of the body Identification

3.2.2 The Initial Left and Right Boundary Points of the Lung Identification

These points are identified by using the y-coordinate of the initial center point of the body as a reference row to find any pixels along the same row whose gradients of intensity are not equal to 0 by calculating outward from the y-coordinate of the initial center point of the body as shown in Figure 14.

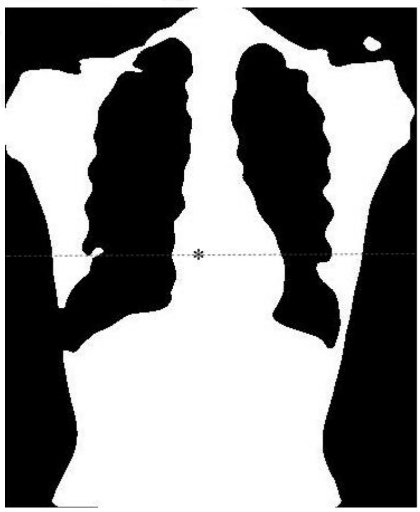

Figure 14 Selected row

These gradients might occur more than what is expected so the selection is constrained as follows:

- First gradient that occurs from the boundary of an image.
- First and second gradients that occur from the initial center point of the body.

The procedure is represented in Figure 15.

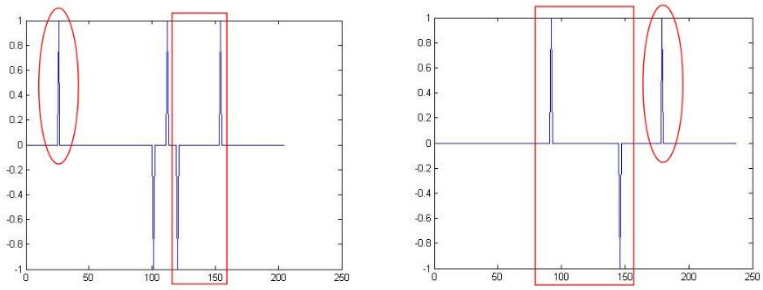

Figure 15 Selected gradient

The proper gradients are defined as the initial left and right boundary points.

There are altogether six boundary points which represent the left and the right boundaries. Four pixels represent the left and the right boundaries of each lung and two pixels represent the left and the right boundaries of the body. These points are shown as '+' in Figure 17.

3.2.3 The Initial Upper and Lower Boundary Points of the Lung Identification

These points are identified by finding the upper and the lower y-coordinates of the midpoints between the left and the right boundary points of both sides of the lung whose gradients are not equal to 0. The upper boundary point is defined at the lower of the upper y-coordinates of both sides of the lung and the lower boundary point is defined at the lower y-coordinate of the right lung only because the heart at the left lung might interfere the result as shown in Figure 16.

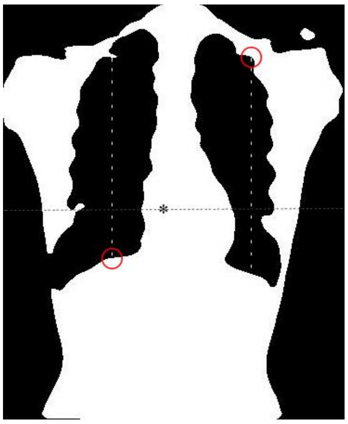

Figure 16 Initial upper and lower boundary points of the lung Identification

These points are shown as ‘x’ in Figure 17.

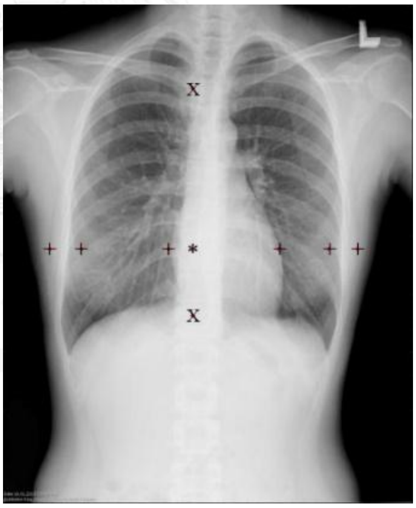

Figure 17 Final results of initial boundary point identification

3.3 Cardiac and Thoracic Diameter Measurement

Since the cardio-thoracic ratio is computed by dividing the cardiac diameter (CD) by the thoracic diameter (TD), the next process is to measure the cardiac diameter. Because the heart is non-rigid and asymmetry, the proposed cardiac diameter measurement divides the heart into two sides: the left and the right. It then finds the widest part of the heart on the left and the widest part of the heart on the right separately. The summation of these two values becomes the cardiac diameter. In order to find the widest parts on each side of the heart, the proposed cardiac diameter measurement computes the maximum distances from the center of the body which are the vertical lines that pass through the initial center point of the body to the left side and the right side of the heart.

3.3.1 Measurement on the Left Side of the Heart

- Extract the region of the whole thoracic cage from the enhanced gray scale image by using the initial upper, lower, left and right boundary points obtained from 3.3.2. The extracted region is shown in Figure 18(a).
- Extract the region of the left thoracic cage by segmenting the left side of the thoracic cage from the previous step. The extracted region is shown in Figure 18(b).

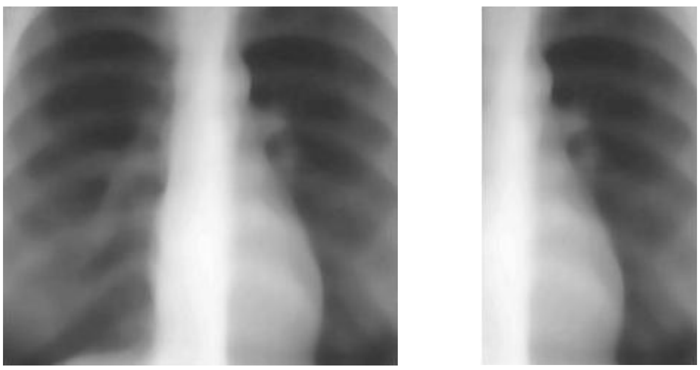

(a) Whole thoracic cage (b) Left thoracic cage

Figure 18 Extracted region of the left side of the heart

- Compute the average intensity of the whole thoracic cage and the average intensity of the left thoracic cage. Set the threshold value to equal to the minimum average intensity from these two values.
- Convert an image of the left thoracic cage to a binary image using the threshold value previously obtained.
- Detect the boundary on the left side of the heart by scanning along the vertical line that passes through the IC point to find the first pixel whose gradient is not equal to 0.
- Detect the left boundary of the heart by using Density-based spatial clustering of applications with noise (DBSCAN) [9] to remove noise from the boundary.
- Connect the left boundary of the heart by using non-linear least square approximation as shown in equations. (1), (2) and (3).

$$E = \sum_{i=1}^{m}[y_i - P_n(x_i)]^2 \tag{1}$$

where $P_n(x_i)$ is a polynomial equation, y_i are data and E represents the sum of errors of m data which consists of x_i,y_i when i = 1,2,..., m.

$$\frac{\partial E}{\partial a_j} = 0 \tag{2}$$

In order to minimize the sum of the least square, the gradient is set to zero where a_j are the coefficients of a polynomial $P(x)$ of degree n, j= 1,2,..., n, and the results will be used in equation (3).

$$P_n(x) = a_0 + a_1x + \cdots + a_{n-1}x^{n-1} + a_nx^n \tag{3}$$

- Find the widest part on the left side of the heart by finding the maximum distance along the vertical line from the center of the body to the left boundary of the heart. The left boundary and its widest part, LCD, are shown in Figure 19.

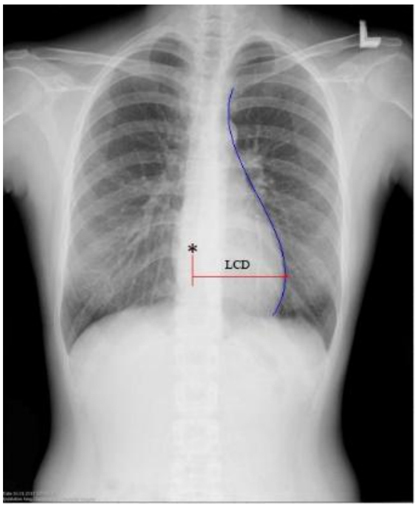

Figure 19 Widest part on the left side of the heart

3.3.2 Measurement on the Right Side of the Heart.

- Extract the region of the right thoracic cage from the enhanced gray scale by using the initial upper, lower, left and right boundary points obtained from 3.3.2. The extracted region is shown in Figure 20.

Figure 20 Extracted region on the right side of the heart

- Quantize an 8-bit gray scale image of the right thoracic cage to a 4-bit gray scale image and plot a histogram.
- Find the valley in the histogram whose area is the maximum. The area can be computed by

$$valley = \int_a^b \big(c - f(x)\big)dx \qquad (4)$$

where $f(x)$ is an equation of the graph, c represents the highest point of the valley and $[a, b]$ represent the range of intensity of the valley. Then the threshold value, t, is set to equal to the intensity of the local minimum of the valley as shown in Figure 21.

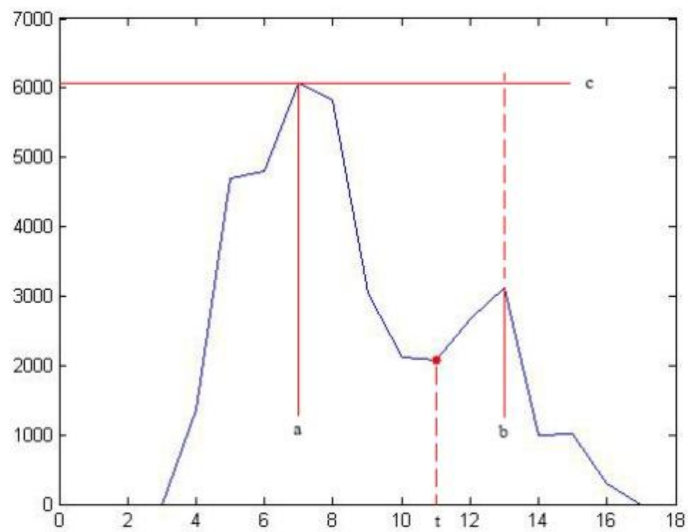

Figure 21 Local minimum calculation

- Convert an image of the right thoracic cage to a binary image using the threshold value previously obtained.
- Detect the right boundary of the heart by using DBSCAN to remove noise from the boundary.
- Connect the right boundary of the heart by using the same non-linear least square approximation.
- Find the widest part on the right side of the heart by finding the maximum distance along the vertical line from the center of the

body to the right boundary of the heart. The right boundary and its widest part, RCD, are shown in Fig. 22.

-

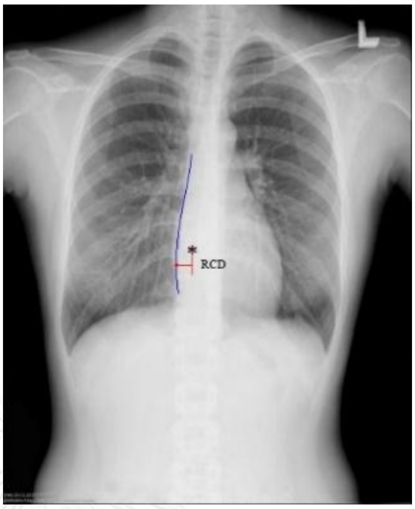

Figure 22 Widest part on the right side of the heart

3.3.3 Thoracic Diameter Measurement.

The diameter of the thoracic is measured from a binary image by calculating the distance from the left to the right boundary of the thoracic cage along each row. The maximum diameter, TD, is shown in Figure 23.

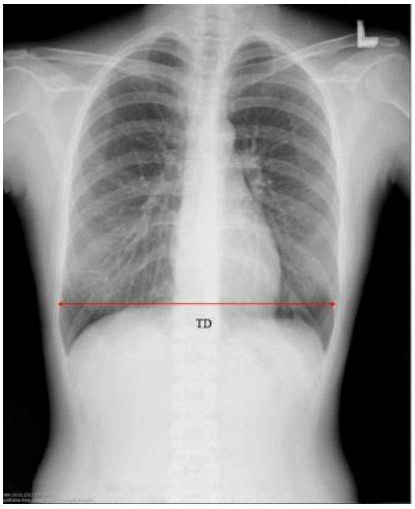

Figure 23 Maximum diameter of Thoracic cage

Next, the cardio-thoracic ratio (CTR) can be calculated by

$$CTR = \frac{CD}{TD} \quad (5)$$

where $CD = LCD + RCD$ as shown in Figure 24.

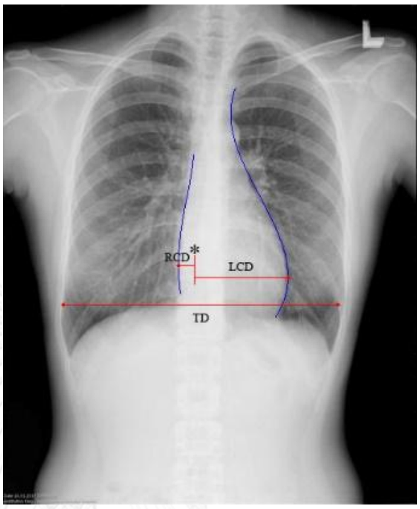

Figure 24 Cardio-Thoracic ratio calculation process

CHAPTER IV

EXPERIMENTAL RESULTS AND DISCUSSION

The proposed method was tested on a set of 523 chest radiographs which were taken in posterior-anterior position. All images are collected from King Chulalongkorn Memorial Hospital, Bangkok, Thailand. The format of the original images is DICOM format with the resolution of 2688x2208 pixels.

To validate efficiency of our work, a correlation test using Pearson's linear correlation coefficient is performed between our results and set of numerical measurement results. The first set consists of RCD, LCD, CD, TD and CTR which were measured by the radiologist and the second set which contains the same type of information but were measured by our proposed technique. The correlation results are demonstrated in Table 1.

Table 1 Correlation test results

RCD	LCD	CD	TD	CTR
0.842	0.9018	0.8909	0.9389	0.8129

The comparison results which are used to perform correlation test are displayed in graphs shown in Figures 25, 26, 27, 28 and 29. Also some examples of the result images are displayed in Table 2 and they indicate that the points used to measure cardio-thoracic ratio (CTR) selected by radiologist and the proposed method yield similar numerical results.

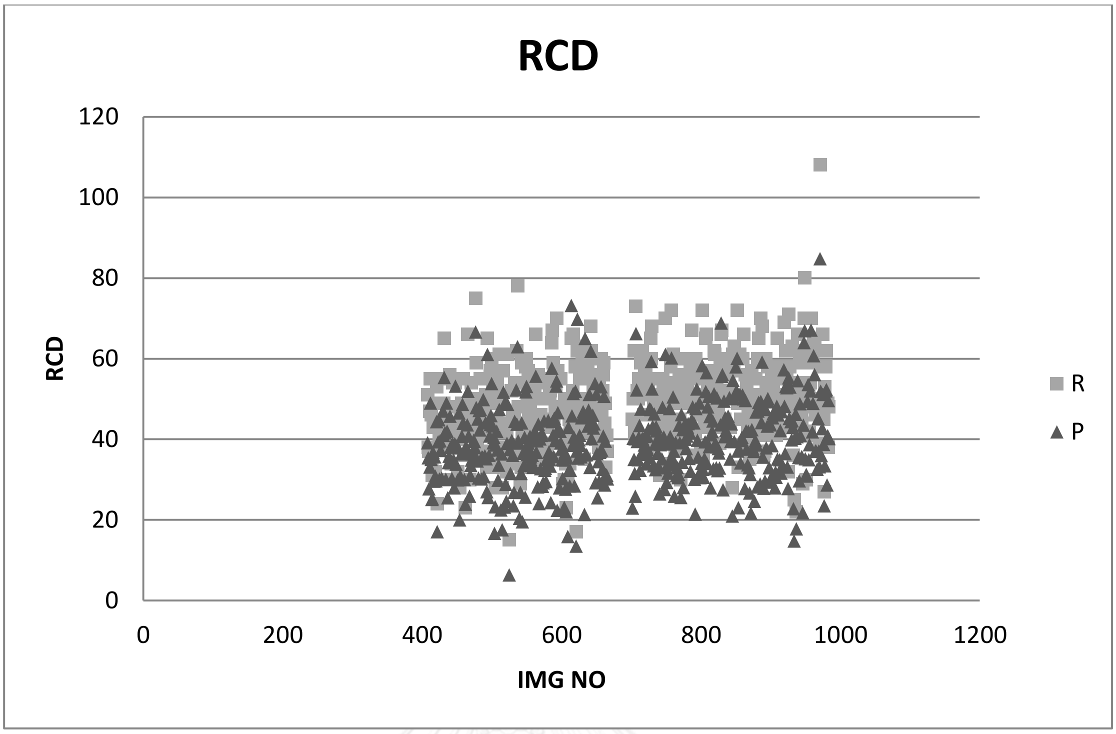

Figure 25 RCD comparison graph

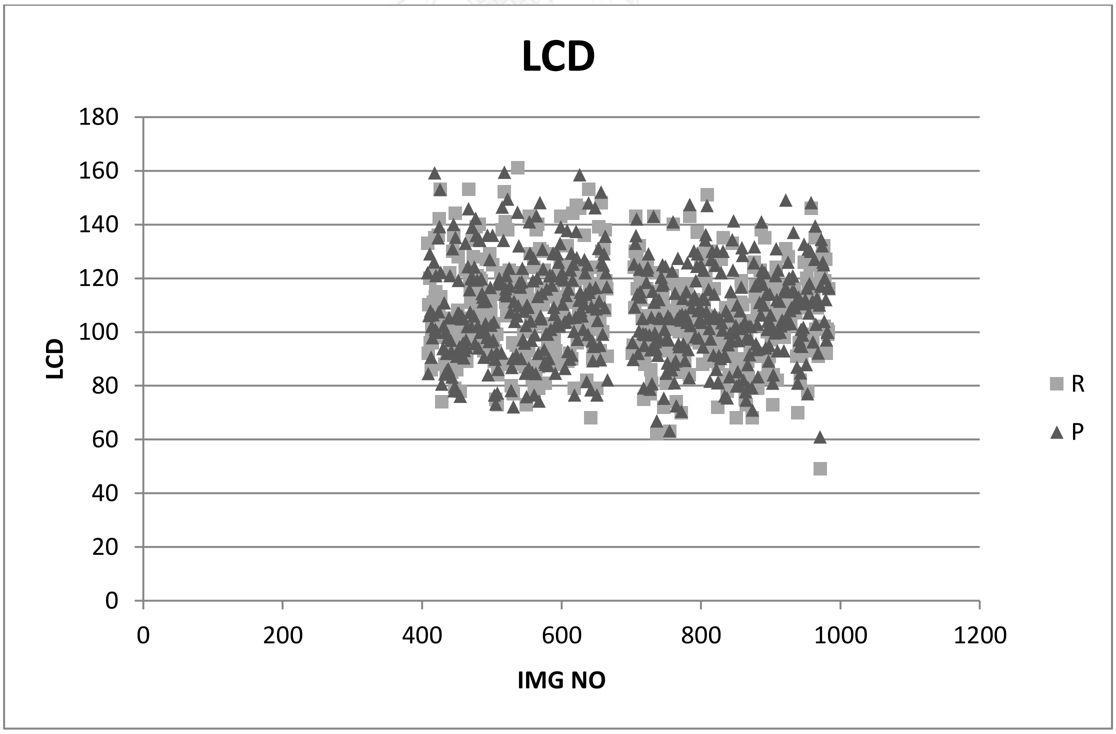

Figure 26 LCD comparison graph

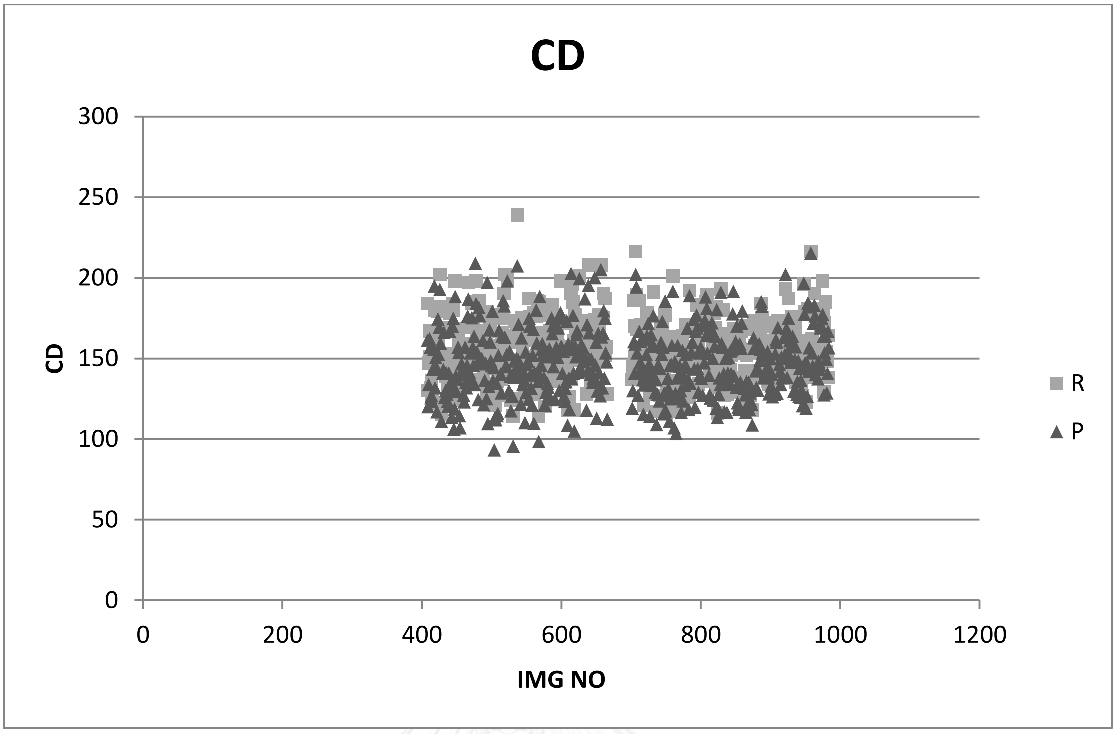

Figure 27 CD comparison graph

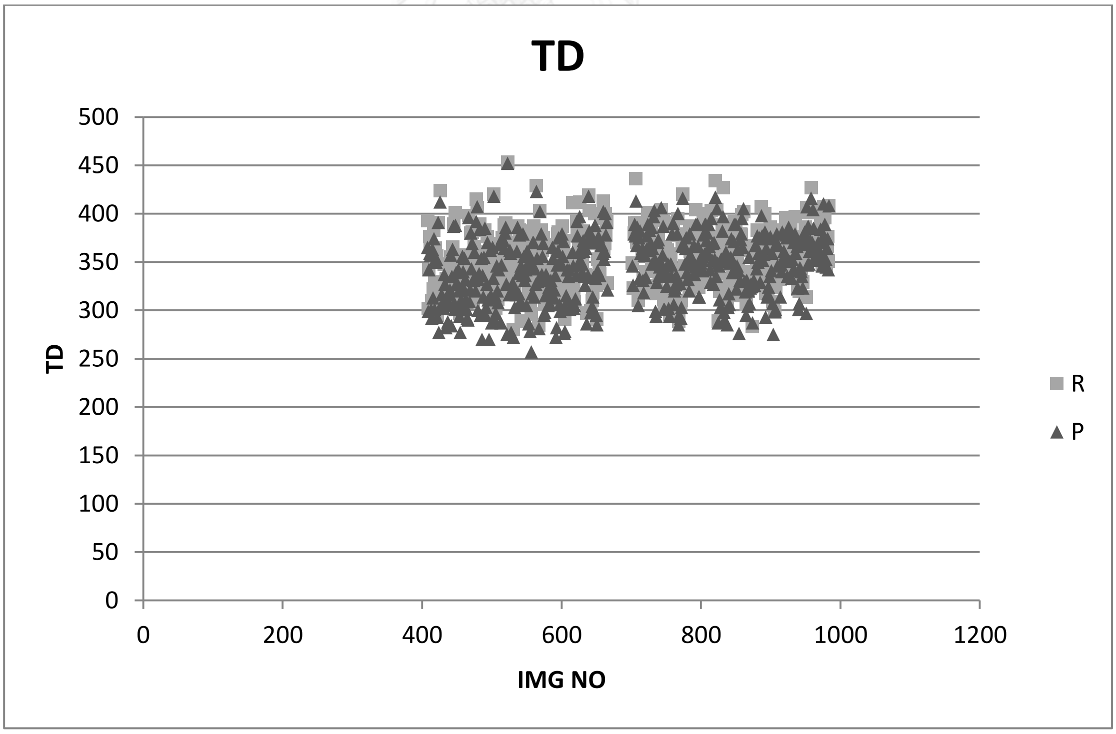

Figure 28 TD comparison graph

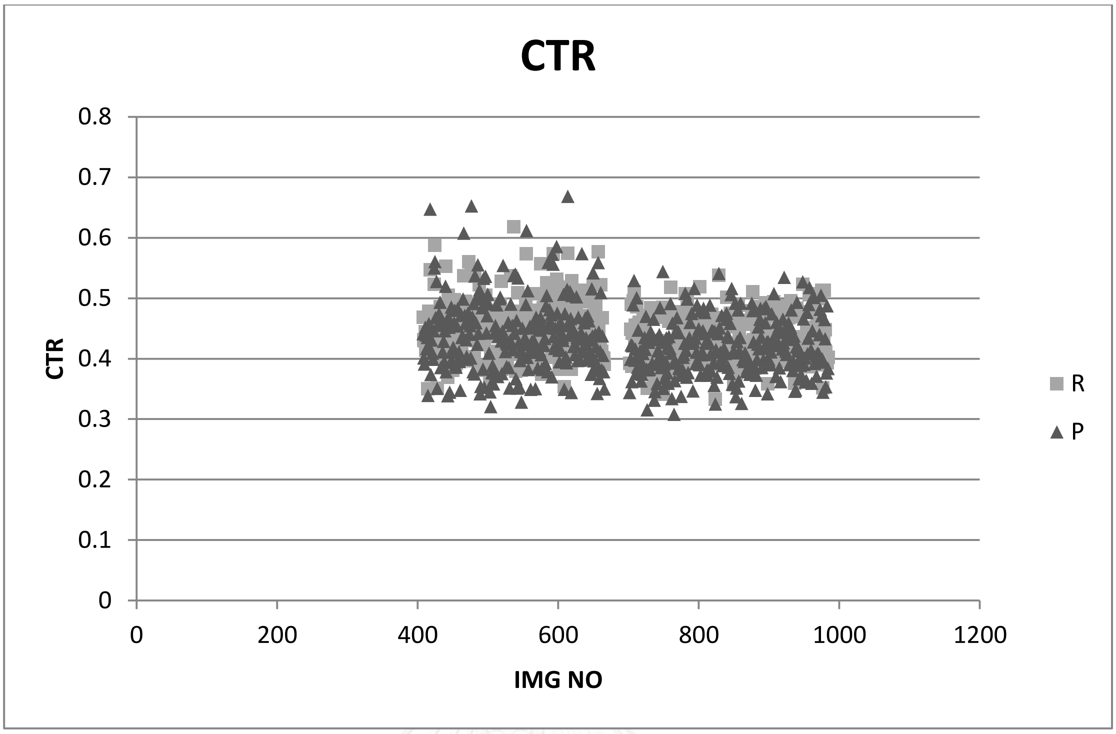

Figure 29 CTR comparison graph

Table 2 Examples of comparison results

IMAGE NO.	The points to measure CTR selected by radiologist.	The points to measure CTR selected by the proposed method.
409	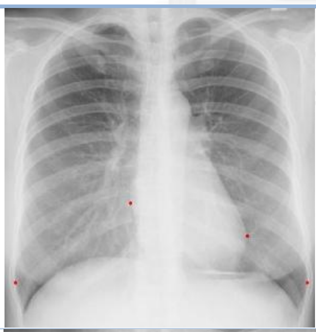	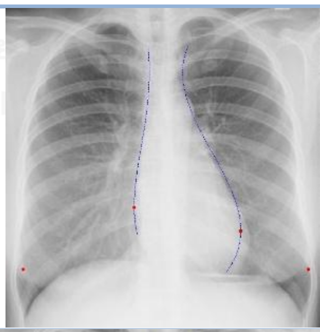
419		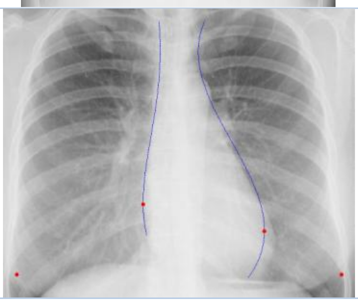

IMAGE NO.	The points to measure CTR selected by radiologist.	The points to measure CTR selected by the proposed method.
425		
771	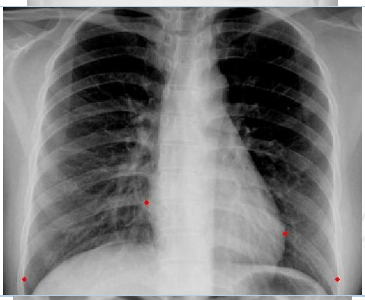	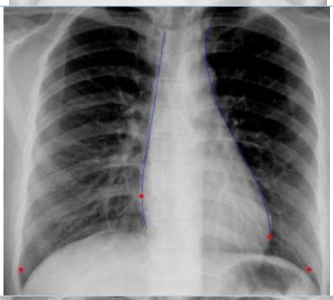
797	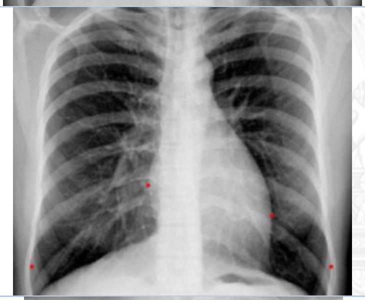	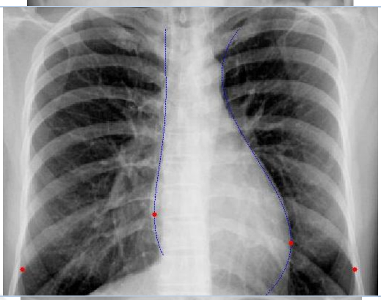
596		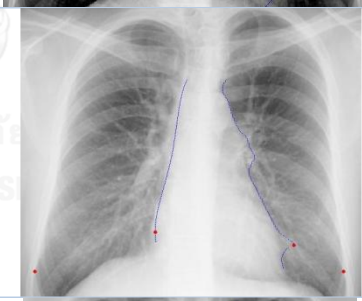
456		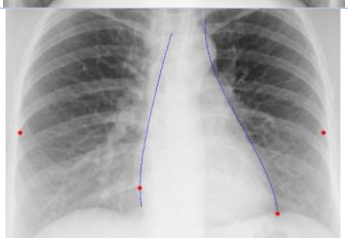
613	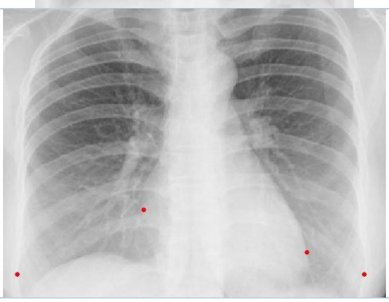	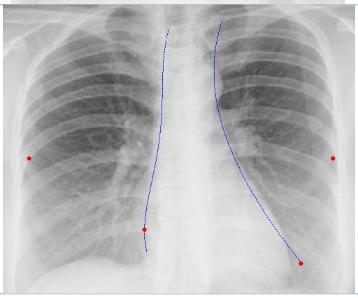

IMAGE NO.	The points to measure CTR selected by radiologist.	The points to measure CTR selected by the proposed method.
623		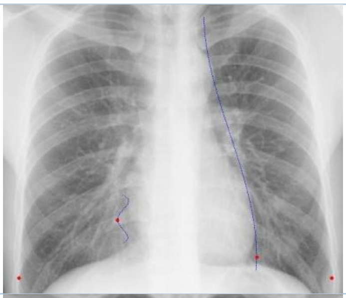
634	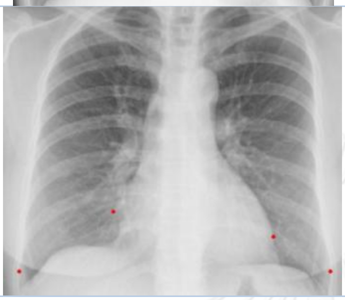	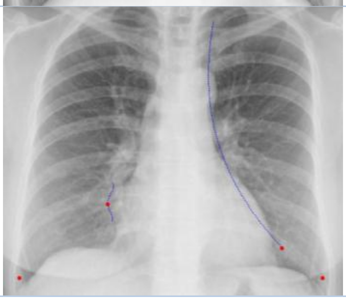

From an observation in the correlation test results in Table 1, the promising outcomes of the proposed method are shown. However it is not yet 100 percent perfect in analyzing or diagnosing the cardio-thoracic ratio (CTR) of the patient due to several reasons. First of all, the points used as a reference data to calculate the cardio-thoracic ratio (CTR) which are pinned by the radiologist are an individual skill thus even for the same chest radiograph but if it is analyzed by different radiologist, the position of the pinned points will be slightly different. Secondly, some of the chest radiographs contain pericardial fat pad or vascular shadow whose intensity values are close to the intensity values of the heart which makes the diagnosis process more intricate and likely to result in an incorrect measurement of the overall data especially in RCD as shown in IMAGE NO: 596, 456, 613, 623 and 634 displayed in Table 2.

CHAPTER V

CONCLUSION

This thesis presents a new method to automatically measure the cardio-thoracic ratio (CTR) from an input image of a Posterior-Anterior chest radiograph by using non-linear least square approximation and local minimum. Then, Pearson's linear correlation coefficient is used to validate the results between two measurements, one from the radiologist and another one from the proposed method, displayed in Table 1. In Table 1, the correlation results of right cardiac diameter (RCD), left cardiac diameter (LCD), cardiac diameter (CD), thoracic diameter (TD) and cardio-thoracic ratio (CTR) measurement show quite a promising trend between two numerical datasets which strongly supported by the example of comparison results demonstrates in Table 2. However, these results can be improved due to some of an incorrect measurement because some of the chest radiographs might contained pericardial fat pad or vascular shadow whose intensities are similar to the heart which is difficult to distinguish and cause the measurement of RCD and LCD to be discrepancy.

For future work, the machine learning and the artificial neural network might be needed in order to increase the correlation results but this procedure may take more time consumption than this proposed methodology.

REFERENCES

1. Longo, D.L. and T.R. Harrison, *Harrison's principles of internal medicine*. 2012, New York: McGraw-Hill.
2. Doi, K., et al., *Computer-aided diagnosis in radiology: potential and pitfalls.* European journal of Radiology, 1999. **31**(2): p. 97-109.
3. Ester, M., et al. *A density-based algorithm for discovering clusters in large spatial databases with noise*. in *Kdd*. 1996.
4. Ilovar, M. and L. Sajn. *Analysis of radiograph and detection of cardiomegaly*. in *MIPRO, 2011 Proceedings of the 34th International Convention*. 2011. IEEE.
5. Danzer, C.S., *The cardiothoracic ratio: an index of cardiac enlargement.* The American Journal of the Medical Sciences, 1919. **157**(4): p. 513-554.
6. Dai Duong, H. and D.T. Tinh. *A texture-based approach to chest radiography segmentation*. in *Control, Automation and Information Sciences (ICCAIS), 2012 International Conference on*. 2012. IEEE.
7. Ishida, T., et al. *Computer-aided diagnosis for detection of cardiomegaly in digital chest radiographs*. in *Medical Imaging*. 2005. International Society for Optics and Photonics.
8. Armato III, S.G., M.L. Giger, and H. MacMahon, *Automated lung segmentation in digitized posteroanterior chest radiographs.* Academic radiology, 1998. **5**(4): p. 245-255.
9. Sezaki, N. and K. Ukena, *Automatic computation of the cardiothoracic ratio with application to mass screening.* Biomedical Engineering, IEEE Transactions on, 1973(4): p. 248-253.
10. Van Ginneken, B., B.M. ter Haar Romeny, and M.A. Viergever, *Computer-aided diagnosis in chest radiography: a survey.* Medical Imaging, IEEE Transactions on, 2001. **20**(12): p. 1228-1241.
11. Van Ginneken, B., M.B. Stegmann, and M. Loog, *Segmentation of anatomical structures in chest radiographs using supervised methods: a comparative study on a public database.* Medical Image Analysis, 2006. **10**(1): p. 19-40.

APPENDICES

APPENDIX A

Cardio-Thoracic Ratio Measurement Using Non-linear Least Square Approximation and Local Minimum

Wasin Poncheewin[1], Monravee Tumkosit, MD[2], Rajalida Lipikorn[1]
[1]Machine Intelligence and Multimedia Information Technology Laboratory, Department of Mathematics and Computer Science, Faculty of Science, Chulalongkorn University, Bangkok, Thailand.
[2]Department of Radiology, Faculty of Medicine,Chulalongkorn University, Bangkok, Thailand.

Abstract

This paper presents a method to automatically measure cardio-thoracic ratio (CTR) from a chest radiographic images using non-linear least square approximation and local minimum. The proposed method consists of initial boundary point identification, cardiac diameter measurement, thoracic diameter measurement and cardio-thoracic ratio measurement. First, the initial boundary points used to approximate the region of thoracic cavity are identified using general human anatomy features. Then the non-linear least square approximation and local minimum are used to detect the heart boundary. Finally, the thoracic cage boundary is detected and the cardio-thoracic ratio can be measured. The proposed method is tested on a set of 255 chest radiographs. The experimental results are evaluated using correlation test between two sets of numerical measurement which are measured by our proposed method and by the radiologists. The evaluation reveals that the correlation result on CTR is about 78%.

Keywords: Chest radiograph, cardio-thoracic ratio, computer-aided diagnosis.

1. Introduction

Radiography is one of the most widely used medical procedures performed to diagnose the insight of human body. Chest radiograph is a useful tool for diagnosing the abnormality that occurs in chest cavity and also is a source to obtain the size of the heart which is one of the most important factors used to indicate many heart diseases including enlarged heart or cardiomegaly [1]. In the past, cardio-thoracic ratio (CTR) was manually measured by radiologists. At the present, computer-aided diagnosis (CAD) system has become much more popular. This technology has improved the way to diagnose many diseases by giving many advantages such as accuracy, time consumption reduction and automation [2] but a fully automated CTR measurement has not yet been able to gain a complete reliability from radiologists.

Various techniques of automated detection of cardiomegaly have been proposed. The study by M. Ilovar and L. Šajn uses edge detection to locate the position of the heart and determine the border of the thoracic cage by drawing a horizontal line toward the end of an image from the points on both sides of the heart boundary which have been calculated as the widest part and finding the brightest intensity [3]. This method of measuring the CTR is not precise according to the actual definition by Danzer, C.S. [4]. Ishida and his colleagues had developed an algorithm that uses histogram analysis and edge detection technique with feature analysis to diagnose the cardiomegaly but it is not yet fully automated [5]. Another novel method was developed by Sezaki Nobuhiko and Ukena Kohji which can compute the CTR within one second but it must be installed on their special instrument [6]. Beside all of the technical work, there are also a survey and a comparative study of other proposed methods that provide useful information [7,8].

The aim of this proposed method is to develop a fully automated CTR measurement technique without the use of training data set which can improve the accuracy and efficiency. The paper is organized as follows: section 2 presents related work and theoretical background, section 3 proposes a new CTR measurement, section 4 provides experimental results, and section 5 gives some discussion and conclusions.

2. Proposed methodology

In order to measure CTR, the radiographic images in DICOM format are converted to gray scale images. The input images are then passed through the proposed method which consists of four main processes: initial boundary point identification, cardiac diameter measurement, thoracic diameter measurement, and CTR measurement.

2.1 Initial boundary point identification

In the first process, histogram equalization and median filter are used to enhance a gray scale image. Then, the average intensity is used as a threshold value to convert a gray scale image to a binary image. Next, the initial boundary points which are used to define the region of lung are identified by the following process.

i) Identify the initial center point (IC) of the body by setting the x-coordinate to equal to the middle column of the white region on the last row of a binary image of each patient which is assumed to represent the patient's body and setting the y-coordinate to be half of the height of an image. The IC point is shown as '*' in Fig. 1.

ii) Identify the initial left and right boundary points (LR) by using the initial center point obtained from previous step. There are altogether six boundary points which represent the left and the right boundaries. Four pixels represent the left and the right boundaries of each lung, and two pixels represent the left and the right boundaries of the body. These six initial boundary points are identified by finding the pixels along the same row as the initial point whose gradients of intensity are not equal to 0. The LR points are shown as '+' in Fig. 1.

iii) Identify the initial upper and lower boundary points (UL) of the lung by finding the lower and upper y-coordinates of the midpoint between the left and the right boundary points of the lung whose gradients are not equal to 0. The UL points are shown as 'x' in Fig. 1.

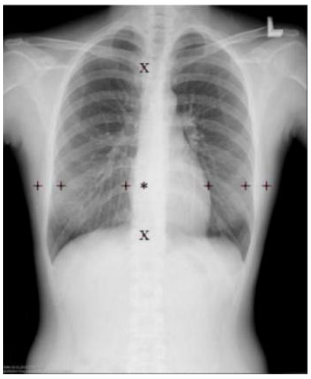

Fig 1: Initial boundary points.

2.2 Cardiac Diameter Measurement

Since the cardio-thoracic ratio is computed by dividing the cardiac diameter (CD) by the thoracic diameter (TD), the next process is to measure cardiac diameter. Because the heart is non-rigid and asymmetry, the proposed cardiac diameter measurement divides the heart into two sides: the left and the right. It then finds the widest part of the heart on the left and the widest part of the heart on the right separately. The summation of these two values becomes the cardiac diameter. In order to find the widest parts on both sides of the heart, the proposed CD measurement computes the maximum distance from the center of the body which is a vertical line that passes through the IC point to the left side of the heart and the maximum distance from the center of the body to the right side of the heart as follows:

2.2.1 Measurement on the left side of the heart

i) Extract the region of the whole thoracic cage from an image by using the initial boundary points (LR and UL points) obtained from the first process. The extracted region is shown in Fig. 2(a).

ii) Extract the region of the left thoracic cage by segmenting the left side of the thoracic cage from the previous step. The extracted region is shown in Fig. 2(b).

iii) Compute the average intensity of the whole thoracic cage and the average intensity of the left thoracic cage. Set the threshold value to equal to the minimum average intensity from these two values.

iv) Convert an image of the left thoracic cage to a binary image using the threshold value obtained from step 3).

v) Detect the boundary on the left side of the heart by scanning along the vertical line that passes through the IC point to find the first pixel whose gradient is not equal to 0.

vi) Detect the left boundary of the heart by using Density-based spatial clustering of applications with noise (DBSCAN) [9] to remove noise from the boundary.

vii) Connect the left boundary of the heart by using non-linear least square approximation as shown in eqn. (1), (2) and (3).

$$E = \sum_{i=1}^{m}[y_i - P_n(x_i)]^2 \tag{1}$$

where E represents the sum of error of m data which consists of x_i,y_i when $i = 1,2,\ldots, m$.

$$\frac{\partial E}{\partial a_j} = 0 \tag{2}$$

In order to minimize the sum of the least square, the gradient is set to zero where a_j is the coefficients of a polynomial $P(x)$ of degree n, j= 1,2,…, n, and the results will be used in eqn.(3).

$$P_n(x) = a_0 + a_1x + \cdots + a_{n-1}x^{n-1} + a_nx^n \tag{3}$$

viii) Find the widest part on the left side of the heart by finding the maximum distance along the vertical line from the center of the body to the left boundary of the heart. The left boundary and its widest part, LCD, are shown in Fig. 2(c).

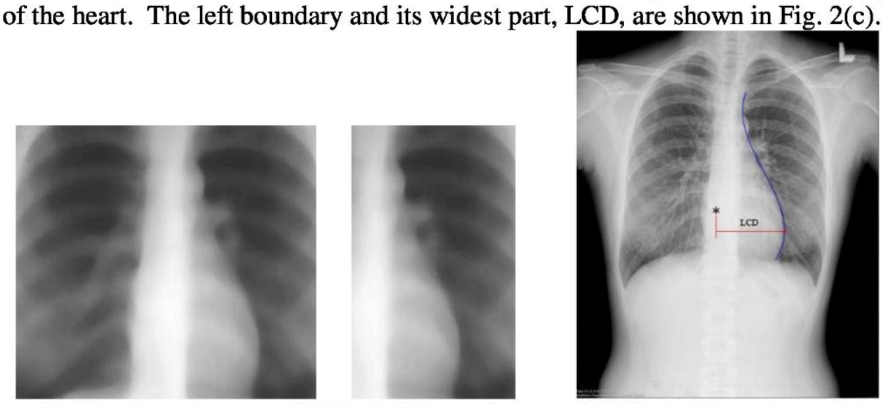

(a) The thoracic cage. (b) The left thoracic cage. (c) The left boundary of the heart and the widest part.

Fig. 2: The thoracic cage, the left thoracic cage and the left boundary of the heart and the widest part.

2.2.2 Measurement on the right side of the heart

i) Extract the region of the right thoracic cage by using the initial boundary points (LR and UL points) obtained from the first process. The extract region is shown in Fig. 3.

ii) Quantize an 8-bit gray scale image of the right thoracic cage to a 4-bit gray scale image and plot a histogram.

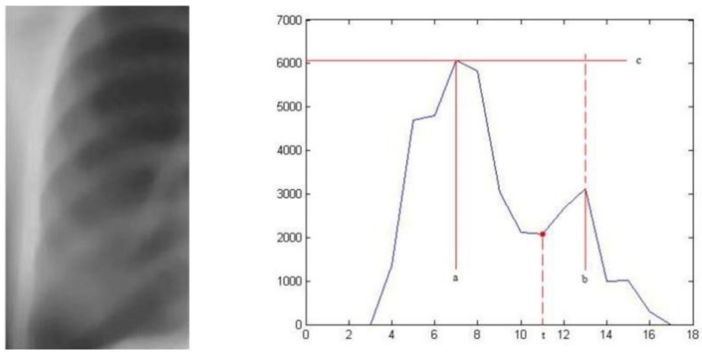

(a) The right thoracic cage. (b) Histogram of the right thoracic cage.

Fig 3: The right thoracic cage and its quantized histogram.

iii) Find the valley in the histogram whose area is the maximum. The area can be computed by

$$valley = \int_a^b \big(c - f(x)\big)dx \tag{4}$$

where c represents the highest point of the valley and $[a, b]$ represent the range of intensity of the valley. Then the threshold value, t, is set to equal to the intensity of the local minimum of the valley as shown in Fig.4.

iv) Convert an image of the right thoracic cage to a binary image using the threshold value obtained from step 3).

v) Detect the right boundary of the heart by using DBSCAN to remove noise from the boundary.

vi) Connect the right boundary of the heart by using the same non-linear least square approximation.

vii) Find the widest part on the right side of the heart by finding the maximum distance along the vertical line from the center of the body to the right boundary of the heart. The right boundary and its widest part, RCD, are shown in Fig. 4.

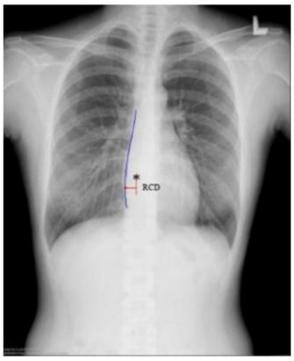

Fig 4: The right boundary of the heart and the widest part.

2.2.3 Thoracic Diameter Measurement

In this process, the diameter of the thoracic cage is computed by first finding the widest part of the thoracic cage and then measuring the distance from the left side to the right side of the thoracic cage. The boundary of the thoracic cage is detected by using the average intensity to convert an image to a binary image. Then the diameter is measured by calculating the distance from the left to the right boundary of the thoracic cage along each row. The maximum diameter, TD, is shown in Fig. 5(a). Then, the CTR can be calculated by

$$CTR = \frac{CD}{TD} \tag{5}$$

where $CD = LCD + RCD$ as shown in Fig. 5(b).

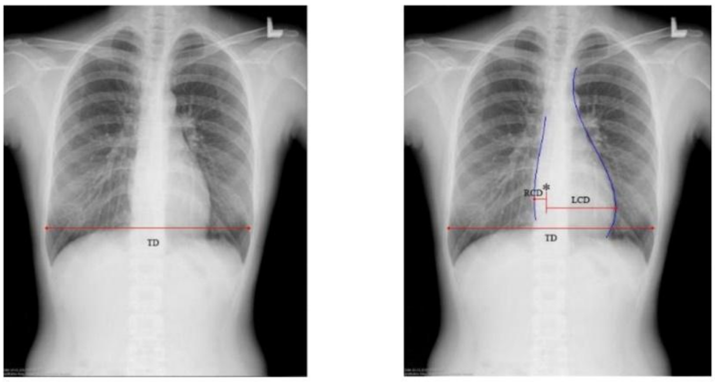

(a) The widest thoracic diameter. (b) The measurement of CTR.

Fig 5: The widest thoracic diameter and the measurement of CTR.

3. Experimental results

The proposed method is tested on a set of 255 chest radiographs which were taken in posterior-anterior position. All images are collected from King Chulalongkorn Memorial Hospital, Bangkok, Thailand. The format of the original images is DICOM format with a resolution of 2688x2208 pixels.

To validate efficiency of our work, a correlation test using Pearson's linear correlation coefficient is performed between two sets of numerical measurement results. The first set consists of RCD, LCD, CD, TD and CTR which were measured by our proposed technique and the second set which contains the same type of information but were measured by the radiologist. Some comparison results are displayed in Fig. 6 and the correlation results are demonstrated in Table 1. It is indicated in Fig. 6 that the numerical results between two datasets are quite similar.

Table 1: Correlation test results

RCD	LCD	CD	TD	CTR
0.7808	0.8957	0.8756	0.9295	0.7849

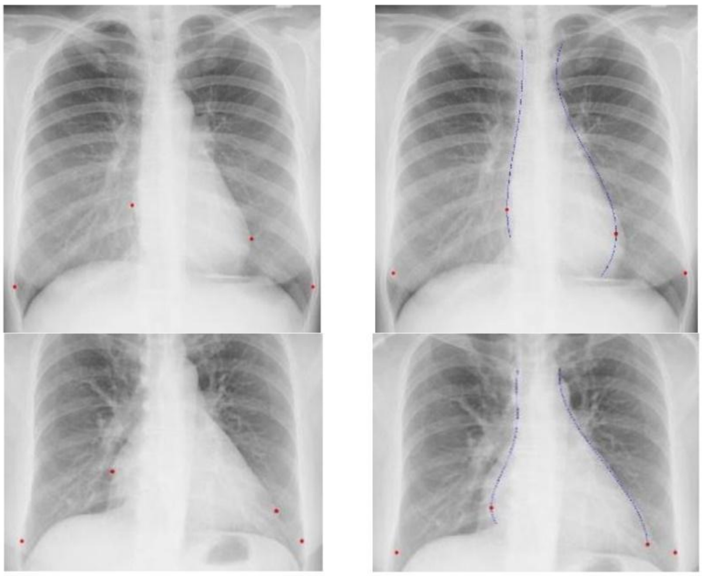

(a) The points to measure CTR selected by the radiologist.

(b) The points to measure CTR selected by the proposed method.

Fig 6: the comparison results

4. Conclusion

This paper presents a new method to automatically measure the CTR from an input image of a Posterior-Anterior chest radiograph by using non-linear least square approximation and local minimum. In Table 1, the results of CTR measurement show quite a promising trend between two numerical datasets. However, these results can be improved because some of the chest radiographs might contained pericardial fat pad or vascular shadow whose intensities are similar to the heart which cause the measurement of RCD and LCD to be discrepancy.

Acknowledgements

This work is supported by Centre of Excellence in Mathematics, Thailand. We would also thank to Petcharleeya Suwanpradit for providing medical images.

References

[1] Longo, D., Fauci, A., Kasper, D., Hauser, S., Jameson, J., & Loscalzo, J., Harrison's Principles of Internal Medicine, (McGraw Hill Professional, 2011, 18 edn. 2011).

[2] Doi, K., MacMahon, H., Katsuragawa, S., Nishikawa, R.M., & Jiang, Y., Computer-aided diagnosis in radiology: potential and pitfalls, European Journal of Radiology, 1999, **31(2)**, pp. 97-109.

[3] Ilovar, M., & Sajn, L., Analysis of radiograph and detection of cardiomegaly, MIPRO, 2011 Proceedings of the 34th International Convention, vol., no., pp.859,863, 23-27 May 2011.

[4] Danzer, C.S., The Cardiothoracic Ratio: An Index of Cardiac Enlargement, The American Journal of the Medical Sciences, 1919, **157(4)**, pp. 513-554.

[5] Ishida, T., Katsuragawa, S., Chida, K., MacMahon, H., & Doi, K., Computer-aided diagnosis for detection of cardiomegaly in digital chest radiographs, Proc. SPIE 5747, Medical Imaging 2005: Image Processing, 914, May. 2005, doi:10.1117/12.595755.

[6] Sezaki, N. & Ukena, K., Automatic Computation of the Cardiothoracic Ratio with Application to Mass Screening, Biomedical Engineering, IEEE Transactions on , vol.BME-20, no.4, pp.248,253, July 1973 doi: 10.1109/TBME.1973.324188.

[7] Van Ginneken, B., ter Haar Romeny, B.M., & Viergever, M.A., Computer-aided diagnosis in chest radiography: a survey, Medical Imaging, IEEE Transactions on , vol.20, no.12, pp.1228,1241, Dec. 2001, doi: 10.1109/42.974918.

[8] Van Ginneken, B., Stegmann, M.B., & Loog, M., Segmentation of anatomical structures in chest radiographs using supervised methods: a comparative study on a public database, Medical Image Analysis, Volume 10, Issue 1, February 2006, Pages 19-40, ISSN 1361-8415.

[9] Ester, M., Kriegel, H. P., Sander, J. & Xu, X., A density-based algorithm for discovering clusters in large spatial databases with noise. Proc. of the Second International Conference on Knowledge Discovery and Data Mining (KDD-96). In Evangelos Simoudis, Jiawei Han, Usama M. Fayyad, AAAI Press, pp. 226–231, 1996.

APPENDIX B

Table B-1 Results of numerical measurement

Abbreviation:

- IMG NO : image file number
- RCD : right cardiac diameter
- LCD : left cardiac diameter
- CD : cardiac diameter
- TD : thoracic cage diameter
- CTR : cardio-thoracic ratio
- R : measured by radiologist
- P : measured by proposed method

*Noted that the unit of these numbers is in pixels.

IMG	RCD		LCD		CD		TD		CTR	
NO	R	P	R	P	R	P	R	P	R	P
408	51	39.15	133	122	184	161.2	393	365	0.468	0.442
409	38	35.43	92	84.53	130	120	302	299	0.43	0.401
410	37	27.67	110	106.1	147	133.8	342	342	0.43	0.391
411	47	33.1	120	129.1	167	162.2	376	359	0.444	0.452
412	55	48.98	96	107.8	151	156.8	365	357	0.414	0.439
413	46	34.96	86	90.56	132	125.5	301	301	0.439	0.417
414	35	25.05	101	102	136	127	310	292	0.439	0.435
415	31	25.26	96	97.87	127	123.1	363	363	0.35	0.339
416	43	36.78	111	106.4	154	143.2	322	313	0.478	0.458
417	43	29.6	121	126	164	155.6	383	374	0.428	0.416
418	45	35.62	135	159.2	180	194.8	329	301	0.547	0.647
419	32	30.9	113	100.9	145	131.8	364	353	0.398	0.373
420	49	29.71	115	120.9	164	150.7	353	350	0.465	0.43
421	53	44.4	101	100	154	144.4	356	353	0.433	0.409
422	24	17.02	98	99.88	122	116.9	295	293	0.414	0.399
423	43	39.37	136	135	179	174.4	391	391	0.458	0.446
424	55	44.87	106	107.5	161	152.4	308	277	0.523	0.55
425	40	30.13	142	139.1	182	169.3	310	302	0.587	0.561
426	49	39.62	153	153	202	192.6	424	412	0.476	0.468
427	38	37.19	113	122.2	151	159.4	323	302	0.467	0.528
428	41	30.32	74	80.57	115	110.9	328	316	0.351	0.351

IMG NO	RCD		LCD		CD		TD		CTR	
	R	P	R	P	R	P	R	P	R	P
430	45	46.96	99	93.86	144	140.8	315	308	0.457	0.457
431	49	40.94	98	102.2	147	143.1	328	302	0.448	0.474
432	65	55.32	104	110.8	169	166.1	348	337	0.486	0.493
433	55	41.62	88	84.42	143	126	327	327	0.437	0.385
434	43	30.08	104	99.92	147	130	321	282	0.458	0.461
435	55	49	84	92	139	141	333	310	0.417	0.455
436	55	42.02	92	85.83	147	127.8	314	311	0.468	0.411
437	30	25.48	95	98	125	123.5	310	288	0.403	0.429
438	40	34.18	91	86.18	131	120.4	324	305	0.404	0.395
439	44	35.75	98	105.2	142	141	332	316	0.428	0.446
440	56	45.73	122	121	178	166.7	322	321	0.553	0.519
441	48	38.02	105	96.96	153	135	355	357	0.431	0.378
442	34	38.43	94	92.87	128	131.3	315	284	0.406	0.462
443	41	30.22	85	83.17	126	113.4	341	335	0.37	0.338
444	54	38.98	130	131	184	170	365	363	0.504	0.468
445	44	34.88	136	140	180	174.9	389	387	0.463	0.452
446	41	27.92	86	78.13	127	106	311	308	0.408	0.344
447	48	38.87	79	79.82	127	118.7	304	301	0.418	0.394
448	54	53.19	144	135.2	198	188.3	401	388	0.494	0.485
449	43	33.84	102	105.3	145	139.1	342	339	0.424	0.41
450	43	38.41	86	90.94	129	129.3	339	328	0.381	0.394
451	32	29.93	108	106.9	140	136.8	323	327	0.433	0.418
452	40	37.87	128	119.1	168	157	338	342	0.497	0.459
453	55	46.49	105	107	160	153.5	339	320	0.472	0.48
454	28	20.02	99	94.52	127	114.5	297	294	0.428	0.39
455	46	30.88	78	76.02	124	106.9	316	277	0.392	0.386
456	42	36.35	102	104.9	144	141.2	332	311	0.434	0.454
457	49	40.68	105	106	154	146.7	317	304	0.486	0.483
458	55	48.63	98	93.08	153	141.7	356	356	0.43	0.398

IMG NO	RCD		LCD		CD		TD		CTR	
	R	P	R	P	R	P	R	P	R	P
459	55	43.99	102	95.85	157	139.8	343	340	0.458	0.411
460	36	36.89	97	90.37	133	127.3	322	322	0.413	0.395
461	43	29.97	99	93.06	142	123	357	354	0.398	0.348
462	23	23.91	123	133	146	156.9	339	332	0.431	0.473
463	41	38.19	97	97.01	138	135.2	337	311	0.409	0.435
464	45	37.6	89	94.18	134	131.8	308	301	0.435	0.438
465	49	43.55	101	102	150	145.6	325	292	0.462	0.498
466	66	51.88	103	124.3	169	176.2	315	290	0.537	0.608
467	44	40.79	153	145.9	197	186.7	398	396	0.495	0.471
468	30	25.83	119	115.7	149	141.5	311	309	0.479	0.458
469	43	31.02	116	107.3	159	138.4	322	321	0.494	0.431
470	42	33.52	111	119.8	153	153.3	380	380	0.403	0.404
471	54	34.82	100	102	154	136.8	347	343	0.444	0.399
472	50	36.31	134	138.9	184	175.2	381	369	0.483	0.475
473	45	37	128	119.8	173	156.8	309	331	0.56	0.474
474	46	39.73	105	106	151	145.7	333	331	0.453	0.44
475	45	39.45	114	124.2	159	163.6	366	360	0.434	0.454
476	50	37.92	100	95.71	150	133.6	337	333	0.445	0.401
477	75	66.62	110	142.2	185	208.9	342	320	0.541	0.653
478	59	47.86	139	136	198	183.9	415	392	0.477	0.469
479	40	34.63	121	119.3	161	153.9	406	407	0.397	0.378
480	48	45	110	102.3	158	147.3	334	300	0.473	0.491
481	42	30.4	95	94.04	137	124.4	342	332	0.401	0.375
482	46	47.14	140	134.4	186	181.6	347	338	0.536	0.537
483	47	42.27	120	134.1	167	176.4	389	384	0.429	0.459
484	55	47.39	100	99.85	155	147.2	324	295	0.478	0.499
485	43	30.15	119	119.7	162	149.9	360	354	0.45	0.423
486	36	35.6	114	114.2	150	149.8	316	270	0.475	0.555
487	46	35.48	109	113	155	148.5	340	336	0.456	0.442

IMG NO	RCD R	RCD P	LCD R	LCD P	CD R	CD P	TD R	TD P	CTR R	CTR P
488	55	49.81	111	111.3	166	161.1	318	314	0.522	0.513
489	45	30.71	93	90.6	138	121.3	358	355	0.385	0.342
490	48	35.85	98	100.4	146	136.3	383	385	0.381	0.354
491	51	44.02	104	103.1	155	147.1	330	295	0.47	0.499
492	37	35.13	127	111.6	164	146.7	336	303	0.488	0.484
493	33	27.01	95	98	128	125	330	327	0.388	0.382
494	65	61.06	114	136	179	197.1	376	370	0.476	0.533
495	37	25.55	97	84.05	134	109.6	316	311	0.424	0.352
496	41	36.04	109	96.4	150	132.4	304	270	0.493	0.491
497	43	40.81	129	126.9	172	167.8	341	313	0.504	0.536
498	57	43.62	110	116.5	167	160.1	362	362	0.461	0.442
499	50	45.84	108	102.5	158	148.4	359	315	0.44	0.471
500	60	53.77	93	91.58	153	145.4	324	287	0.472	0.506
501	52	43.33	125	135.9	177	179.2	369	365	0.48	0.491
502	54	39.12	96	97	150	136.1	339	333	0.442	0.409
503	51	40.5	103	103.7	154	144.2	420	418	0.367	0.345
504	33	16.63	89	76.6	122	93.23	298	291	0.409	0.32
505	28	23.22	93	89.85	121	113.1	323	315	0.375	0.359
506	49	38.58	75	73.25	124	111.8	302	297	0.411	0.377
507	45	41.94	99	92.52	144	134.5	350	346	0.411	0.389
508	54	37.3	73	77.26	127	114.6	322	320	0.394	0.358
509	52	29.81	84	86.05	136	115.9	312	308	0.436	0.376
510	44	33.53	114	118.2	158	151.7	345	342	0.458	0.444
511	61	47.37	115	119.9	176	167.3	367	368	0.48	0.455
513	34	22.47	122	117.8	156	140.3	327	287	0.477	0.489
514	49	36.38	88	92.09	137	128.5	352	347	0.389	0.37
515	28	17.53	138	146.4	166	164	375	375	0.443	0.437
517	57	51.67	118	134	175	185.7	374	372	0.468	0.499
518	38	23.19	152	159.4	190	182.6	388	364	0.49	0.502

IMG NO	RCD		LCD		CD		TD		CTR	
	R	P	R	P	R	P	R	P	R	P
519	61	49.11	141	114	202	163.1	383	380	0.527	0.429
520	38	28.78	111	116.1	149	144.9	390	386	0.382	0.375
521	32	24.63	117	121	149	145.6	330	327	0.452	0.445
522	42	38.97	106	113.5	148	152.4	316	275	0.468	0.554
523	61	48.66	138	149.4	199	198.1	453	452	0.439	0.438
525	15	6.313	123	123.7	138	130	341	316	0.405	0.411
526	44	37.43	120	117	164	154.4	368	362	0.446	0.427
527	34	31.47	106	107.4	140	138.9	362	359	0.387	0.387
528	44	39.23	80	78.23	124	117.5	317	277	0.391	0.424
529	52	39.71	88	86.81	140	126.5	321	275	0.436	0.46
530	47	36	96	90.28	143	126.3	335	328	0.427	0.385
531	37	23.46	77	72.12	114	95.58	280	272	0.407	0.351
532	45	26.78	115	111.4	160	138.2	346	321	0.462	0.43
533	54	44.46	119	104	173	148.4	322	303	0.537	0.49
535	54	52.21	95	91.58	149	143.8	360	316	0.414	0.455
536	62	43.7	108	106	170	149.7	370	361	0.459	0.415
537	78	62.92	161	144.5	239	207.4	387	386	0.618	0.537
538	48	39.61	113	109.8	161	149.4	366	338	0.44	0.442
539	44	39.05	116	132	160	171	335	317	0.478	0.54
540	37	20.39	108	118.3	145	138.7	383	378	0.379	0.367
541	29	26.8	118	116.7	147	143.5	334	310	0.44	0.463
542	33	31.52	92	90.08	125	121.6	289	346	0.433	0.351
543	59	44.07	116	118.6	175	162.7	344	305	0.509	0.533
544	42	19.48	122	123.7	164	143.1	349	336	0.47	0.426
545	40	36.51	116	97.17	156	133.7	382	379	0.408	0.353
546	48	33.48	100	107.8	148	141.3	360	356	0.411	0.397
547	54	40.5	88	95.79	142	136.3	337	331	0.421	0.412
548	42	25.59	87	84.6	129	110.2	339	336	0.381	0.328
549	58	51.71	93	102.3	151	154.1	346	342	0.436	0.45

IMG NO	RCD		LCD		CD		TD		CTR	
	R	P	R	P	R	P	R	P	R	P
550	60	53.1	73	75.95	133	129.1	312	305	0.426	0.423
551	51	36.18	115	110	166	146.1	365	361	0.455	0.405
552	57	39.07	112	109.2	169	148.3	378	349	0.447	0.425
553	46	37.8	93	86.51	139	124.3	323	286	0.43	0.435
554	44	33.73	143	141	187	174.7	377	357	0.496	0.489
555	47	40.73	129	129.3	176	170	307	278	0.573	0.612
556	38	35.6	105	104	143	139.6	348	347	0.411	0.402
557	40	34.68	101	96.9	141	131.6	296	257	0.476	0.512
558	45	36.04	83	85	128	121	331	317	0.387	0.382
559	40	33	111	119	151	152	377	370	0.401	0.411
560	54	40.37	124	127.4	178	167.8	387	370	0.46	0.454
561	50	33.18	78	76.49	128	109.7	320	314	0.4	0.349
562	53	42.01	108	98.97	161	141	354	343	0.455	0.411
563	66	55.63	84	84.54	150	140.2	331	327	0.453	0.429
564	38	36.73	138	143.2	176	180	429	423	0.41	0.425
565	40	39.56	110	120	150	159.6	359	354	0.418	0.451
566	46	28.13	140	113.2	186	141.4	367	330	0.507	0.428
567	56	43.75	87	92.07	143	135.8	335	331	0.427	0.41
568	35	24.07	79	74.29	114	98.36	284	281	0.401	0.35
569	54	40.1	131	148.2	185	188.3	403	402	0.459	0.468
570	46	32.71	103	106	149	138.7	349	332	0.427	0.418
571	54	40.91	112	104.9	166	145.8	383	379	0.433	0.385
572	50	41.47	115	114.3	165	155.8	344	337	0.48	0.462
573	35	28.35	130	130.7	165	159.1	362	356	0.456	0.447
574	50	29.17	110	123.5	160	152.6	375	369	0.427	0.414
575	54	44.53	123	93.49	177	138	318	295	0.557	0.468
576	38	32.31	92	88.78	130	121.1	306	298	0.425	0.406
577	39	32.78	81	88	120	120.8	321	315	0.374	0.383
578	36	29.5	113	99.32	149	128.8	339	337	0.44	0.382

IMG	RCD		LCD		CD		TD		CTR	
NO	R	P	R	P	R	P	R	P	R	P
579	45	35.02	116	116	161	151	333	335	0.483	0.451
580	43	35.47	97	99.13	140	134.6	329	319	0.426	0.422
581	50	44.66	102	87.46	152	132.1	313	305	0.486	0.433
582	55	36.86	94	90.15	149	127	329	324	0.453	0.392
583	51	34.92	115	120.9	166	155.9	327	320	0.508	0.487
584	52	33.33	115	120.9	167	154.2	318	306	0.525	0.504
585	39	24.25	103	101	142	125.3	334	331	0.425	0.378
586	64	57.62	101	117.4	165	175.1	338	313	0.488	0.559
587	67	44.33	116	121	183	165.3	368	365	0.497	0.453
588	59	41.02	115	129.3	174	170.3	366	354	0.475	0.481
589	45	35.72	129	109.1	174	144.9	344	314	0.506	0.461
590	55	45.22	98	106.5	153	151.7	340	321	0.45	0.473
591	48	39.72	88	84.63	136	124.3	338	336	0.402	0.37
592	53	53.17	93	102.6	146	155.8	313	272	0.466	0.573
593	70	54.41	106	102.4	176	156.8	307	282	0.573	0.556
594	39	22.37	121	129.1	160	151.5	357	347	0.448	0.436
595	57	46.56	110	104	167	150.6	379	361	0.441	0.417
596	47	42.8	111	126	158	168.8	381	375	0.415	0.45
597	35	27.96	102	102.1	137	130.1	310	306	0.442	0.425
598	48	42.02	125	132.9	173	174.9	326	299	0.531	0.585
599	55	39.16	143	139	198	178.2	381	375	0.52	0.475
600	48	37.54	124	120	172	157.5	348	348	0.494	0.453
601	47	34.9	110	122	157	156.9	387	379	0.406	0.414
602	29	30.26	108	110.3	137	140.6	358	356	0.383	0.395
603	41	34.86	113	119.4	154	154.3	372	371	0.414	0.416
604	30	23.1	105	103.5	135	126.6	300	276	0.45	0.459
605	50	36.72	89	86.41	139	123.1	291	278	0.478	0.443
606	34	27.59	111	103.8	145	131.4	334	302	0.434	0.435
607	23	21.97	119	113.6	142	135.5	321	315	0.442	0.43

IMG	RCD		LCD		CD		TD		CTR	
NO	R	P	R	P	R	P	R	P	R	P
608	40	35.39	132	137.7	172	173.1	344	342	0.5	0.506
609	29	15.87	89	92.73	118	108.6	334	311	0.353	0.349
610	39	42.91	117	116	156	158.9	344	335	0.453	0.474
611	45	32.39	104	105.2	149	137.6	352	342	0.423	0.402
612	34	28.38	92	89.92	126	118.3	309	301	0.408	0.393
613	43	32.28	111	123.1	154	155.4	327	302	0.471	0.515
614	65	73.21	125	129.3	190	202.6	331	303	0.574	0.668
615	48	45.77	90	91.48	138	137.3	314	302	0.439	0.454
616	52	38.51	144	119.3	196	157.8	411	360	0.477	0.438
617	66	51.34	119	125.2	185	176.6	357	346	0.518	0.51
618	49	40.58	112	100.2	161	140.8	323	302	0.498	0.466
619	39	28.44	79	76.51	118	104.9	309	305	0.382	0.344
620	58	51.87	119	105.4	177	157.3	335	312	0.528	0.504
621	17	13.52	147	137.4	164	150.9	350	336	0.469	0.449
622	46	37.07	123	127.6	169	164.6	393	392	0.43	0.42
623	62	69.8	96	97.32	158	167.1	378	377	0.418	0.443
624	63	35.29	99	106.1	162	141.4	352	348	0.46	0.406
625	58	39.84	109	111.8	167	151.6	365	360	0.458	0.421
626	55	40.96	146	158.5	201	199.4	412	397	0.488	0.502
627	48	38.5	112	114.8	160	153.3	348	352	0.46	0.436
628	42	35.66	107	108	149	143.7	359	362	0.415	0.397
629	50	45.28	103	113.1	153	158.4	361	338	0.424	0.469
630	59	45.79	97	106	156	151.8	351	348	0.444	0.436
631	58	46.81	101	101	159	147.8	382	372	0.416	0.397
632	59	45.56	105	110.5	164	156.1	371	361	0.442	0.432
633	35	21.34	136	126.9	171	148.2	335	335	0.51	0.442
634	62	64.97	111	122	173	187	337	326	0.513	0.574
635	42	36.12	123	114	165	150.1	374	364	0.441	0.412
636	46	36.21	82	81.59	128	117.8	297	286	0.431	0.412

IMG NO	RCD		LCD		CD		TD		CTR	
	R	P	R	P	R	P	R	P	R	P
637	49	45.8	120	125	169	170.8	372	372	0.454	0.459
638	59	43.22	99	99	158	142.2	336	336	0.47	0.423
639	55	47.22	153	148	208	195.2	419	418	0.496	0.467
640	62	51.13	111	114.8	173	165.9	403	382	0.429	0.434
641	43	32.97	118	116.2	161	149.2	379	374	0.425	0.399
642	68	61.81	68	78.46	136	140.3	300	298	0.453	0.471
643	62	40.17	101	109.4	163	149.5	374	374	0.436	0.4
644	49	44.01	104	96.62	153	140.6	310	304	0.494	0.463
645	56	45.96	90	89.23	146	135.2	318	314	0.459	0.431
646	52	42.8	92	94.68	144	137.5	335	334	0.43	0.412
647	56	43.78	95	94.62	151	138.4	380	370	0.397	0.374
648	60	53.85	114	146.2	174	200	400	388	0.435	0.516
649	40	29.18	124	116.6	164	145.8	369	333	0.444	0.438
650	60	51.22	110	108.6	170	159.8	326	295	0.521	0.542
651	54	36.4	79	76.58	133	113	291	285	0.457	0.396
652	42	25.45	117	104.3	159	129.8	353	341	0.45	0.381
653	38	34.44	139	131	177	165.5	371	376	0.477	0.44
654	54	29.52	113	111.5	167	141	342	336	0.488	0.42
655	46	36.77	103	94.97	149	131.7	338	336	0.441	0.392
656	56	37.03	93	89.67	149	126.7	375	370	0.397	0.342
657	60	52.99	148	152	208	205	361	367	0.576	0.559
658	46	37.31	130	126	176	163.3	395	368	0.446	0.444
659	52	32.53	100	99.21	152	131.7	361	359	0.421	0.367
660	56	40.78	119	124.9	175	165.7	413	402	0.424	0.412
661	59	50.64	131	129	190	179.6	364	353	0.522	0.509
662	44	28.68	108	109	152	137.7	369	361	0.412	0.381
663	49	39.52	138	135.6	187	175.1	400	400	0.468	0.438
664	33	31.3	119	122	152	153.3	379	378	0.401	0.406
665	41	31.06	116	116.8	157	147.9	392	391	0.401	0.378

IMG NO	RCD		LCD		CD		TD		CTR	
	R	P	R	P	R	P	R	P	R	P
666	37	30.12	91	82.15	128	112.3	328	321	0.39	0.35
702	45	22.93	92	96.02	137	119	349	346	0.393	0.344
703	50	40.26	95	89.76	145	130	323	326	0.449	0.399
704	62	35.02	124	125.2	186	160.2	380	379	0.489	0.423
705	42	31.48	109	109.3	151	140.7	390	389	0.387	0.362
706	40	25.85	130	133	170	158.8	385	377	0.442	0.421
707	73	66.19	143	135.8	216	202	436	413	0.495	0.489
708	62	52.2	127	142	189	194.2	370	367	0.511	0.529
709	52	39.41	116	114	168	153.4	391	386	0.43	0.397
710	50	34.9	91	92	141	126.9	310	305	0.455	0.416
711	55	40.46	95	100.3	150	140.8	377	375	0.398	0.375
712	54	43.41	132	123.3	186	166.7	383	333	0.486	0.501
713	51	32.26	119	115	170	147.3	381	382	0.446	0.385
714	59	47.5	112	113	171	160.5	375	359	0.456	0.447
716	62	40.24	105	105	167	145.2	363	364	0.46	0.399
717	52	37.22	98	99.44	150	136.7	334	331	0.449	0.413
718	46	36.24	75	79.12	121	115.4	320	318	0.378	0.363
719	54	38.58	93	95	147	133.6	366	357	0.402	0.374
720	57	40.68	88	99.09	145	139.8	370	357	0.392	0.392
721	57	37.26	101	99.14	158	136.4	340	334	0.465	0.408
722	46	33.88	116	118.5	162	152.3	364	363	0.445	0.42
723	53	40.91	125	123	178	163.9	377	377	0.472	0.435
724	38	37.5	122	124	160	161.5	401	389	0.399	0.415
725	53	42.55	106	129	159	171.6	367	365	0.433	0.47
726	60	47.52	95	98.89	155	146.4	391	383	0.396	0.382
727	51	35.41	77	78.68	128	114.1	365	362	0.351	0.315
728	65	47.41	86	93.38	151	140.8	366	369	0.413	0.382
729	60	59.27	102	105.5	162	164.8	384	386	0.422	0.427
730	68	52.45	81	80.72	149	133.2	352	348	0.423	0.383

IMG NO	RCD R	RCD P	LCD R	LCD P	CD R	CD P	TD R	TD P	CTR R	CTR P
731	51	43.15	100	115.1	151	158.3	372	364	0.406	0.435
732	48	33.39	143	143	191	176.4	395	397	0.484	0.444
733	55	46.26	108	111.1	163	157.4	401	403	0.406	0.391
734	50	38.81	99	99.64	149	138.5	352	353	0.423	0.392
735	39	32.44	99	96.44	138	128.9	343	299	0.402	0.431
736	51	43.1	98	93.7	149	136.8	317	294	0.47	0.465
737	55	42.03	62	66.91	117	108.9	325	329	0.36	0.331
738	49	36.53	94	91.33	143	127.9	376	370	0.38	0.346
739	55	40.51	101	105.3	156	145.8	374	373	0.417	0.391
740	45	33	115	112	160	145	339	336	0.472	0.432
741	31	26.39	96	97.3	127	123.7	343	345	0.37	0.359
742	49	38.64	99	105	148	143.6	349	348	0.424	0.413
743	50	39.53	122	120.3	172	159.8	404	406	0.426	0.394
744	47	35.13	116	117.4	163	152.5	348	347	0.468	0.44
745	55	47.9	114	125	169	172.9	359	357	0.471	0.484
746	53	38.98	110	118	163	157	393	387	0.415	0.406
747	50	40.55	72	75.4	122	116	312	301	0.391	0.385
748	42	27.56	99	101	141	128.6	301	301	0.468	0.427
749	70	61.05	107	124.4	177	185.5	365	341	0.485	0.544
750	34	32.91	81	84.61	115	117.5	337	335	0.341	0.351
751	45	29.31	101	97.78	146	127.1	359	325	0.407	0.391
752	42	38.8	93	88.4	135	127.2	362	346	0.373	0.368
753	42	31.61	108	106	150	137.6	349	348	0.43	0.395
754	39	34.22	106	97.05	145	131.3	350	302	0.414	0.435
755	54	47.6	63	63.22	117	110.8	296	294	0.395	0.377
756	49	40.67	103	105	152	145.7	358	347	0.425	0.42
757	58	39.09	87	86	145	125.1	352	348	0.412	0.359
758	72	60.19	86	86.13	158	146.3	342	335	0.462	0.437
759	42	35.4	121	122.6	163	158	390	379	0.418	0.417

IMG NO	RCD R	RCD P	LCD R	LCD P	CD R	CD P	TD R	TD P	CTR R	CTR P
760	61	50.5	140	141	201	191.5	388	390	0.518	0.491
761	45	37.08	86	88	131	125.1	308	306	0.425	0.409
762	32	25.85	88	81.02	120	106.9	322	320	0.373	0.334
763	37	33.64	118	114.5	155	148.1	326	323	0.475	0.459
764	51	39.23	85	89.22	136	128.5	329	327	0.413	0.393
765	52	30.91	74	72.48	126	103.4	338	336	0.373	0.308
766	50	33.01	106	104.8	156	137.8	377	379	0.414	0.364
767	38	30.48	113	127.4	151	157.9	395	400	0.382	0.395
768	42	31.23	92	95.63	134	126.9	289	285	0.464	0.445
769	56	43.52	100	94.5	156	138	327	295	0.477	0.468
770	45	39.13	111	106.1	156	145.2	330	328	0.473	0.443
771	30	25.57	106	104.4	136	130	307	292	0.443	0.445
772	49	46.11	70	70.45	119	116.6	310	303	0.384	0.385
773	50	34.29	107	106.6	157	140.9	369	367	0.425	0.384
774	54	42.37	110	112.5	164	154.9	420	416	0.39	0.372
775	60	28.01	90	95.56	150	123.6	372	366	0.403	0.338
777	53	43.69	89	89.4	142	133.1	346	348	0.41	0.382
778	51	40	104	106.3	155	146.3	366	364	0.423	0.402
779	56	37.66	115	115	171	152.7	379	375	0.451	0.407
780	52	40.78	104	103.5	156	144.3	342	339	0.456	0.426
781	53	43.04	118	125.7	171	168.7	337	332	0.507	0.508
782	60	43.88	97	93.49	157	137.4	337	332	0.466	0.414
783	42	35.24	84	82.92	126	118.2	321	320	0.393	0.369
784	49	41.57	143	147.4	192	188.9	387	379	0.496	0.498
785	57	32.09	98	102.4	155	134.5	361	357	0.429	0.377
787	67	44.79	100	109	167	153.8	353	354	0.473	0.434
788	59	48.05	112	112	171	160.1	360	348	0.475	0.46
790	36	44.05	112	130.2	148	174.2	378	367	0.392	0.475
791	48	30.09	104	113.3	152	143.4	341	337	0.446	0.426

IMG NO	RCD		LCD		CD		TD		CTR	
	R	P	R	P	R	P	R	P	R	P
792	42	21.44	101	98.18	143	119.6	349	345	0.41	0.347
793	60	47.59	107	119	167	166.6	404	389	0.413	0.428
794	57	52.43	100	124.5	157	176.9	350	343	0.449	0.516
795	46	39.79	137	129	183	168.8	385	389	0.475	0.434
796	51	35.56	107	108	158	143.6	368	366	0.429	0.392
797	36	31.26	98	97.7	134	129	324	314	0.414	0.411
798	57	49	96	104.3	153	153.3	330	314	0.464	0.488
799	55	30.47	110	109	165	139.5	354	353	0.466	0.395
800	37	31.74	127	125	164	156.8	362	349	0.453	0.449
801	48	34.04	101	103.6	149	137.7	356	353	0.419	0.39
802	72	58.26	111	112.3	183	170.5	353	356	0.518	0.479
803	48	32.53	88	94.41	136	126.9	344	341	0.395	0.372
804	36	30.59	129	123	165	153.6	400	378	0.413	0.406
805	43	35.14	109	112.1	152	147.3	357	358	0.426	0.411
806	50	39.33	129	134.2	179	173.5	392	389	0.457	0.446
807	65	51.8	120	136.2	185	188	394	389	0.47	0.483
808	66	56.48	106	107.6	172	164.1	378	372	0.455	0.441
809	38	34	151	147	189	181	398	380	0.475	0.476
810	53	48.04	96	105.1	149	153.1	361	359	0.413	0.427
811	57	50.65	115	115.8	172	166.5	399	389	0.431	0.428
812	47	38.15	101	101.3	148	139.5	371	366	0.399	0.381
813	48	45.67	91	81.72	139	127.4	352	342	0.395	0.372
814	44	27.94	102	97.43	146	125.4	330	329	0.442	0.381
815	52	41.14	130	126.9	182	168	403	395	0.452	0.425
816	54	41.93	93	130	147	171.9	352	352	0.418	0.488
817	56	44.52	100	105.6	156	150.1	375	369	0.416	0.407
818	46	32.69	95	91.4	141	124.1	329	327	0.429	0.38
819	62	51.3	116	114	178	165.3	376	370	0.473	0.447
820	61	50.84	104	106.5	165	157.4	362	353	0.456	0.446

IMG NO	RCD R	RCD P	LCD R	LCD P	CD R	CD P	TD R	TD P	CTR R	CTR P
821	44	38.97	125	124.7	169	163.7	434	417	0.389	0.393
822	43	32.93	89	86.12	132	119	338	335	0.391	0.355
823	55	50.2	127	130	182	180.2	404	405	0.45	0.445
824	44	32.23	72	81.11	116	113.3	349	349	0.332	0.325
825	47	37.66	88	81.36	135	119	289	287	0.467	0.415
826	56	36.57	92	91.16	148	127.7	350	346	0.423	0.369
827	39	32.86	98	105	137	137.9	320	311	0.428	0.443
828	58	43.54	105	90.14	163	133.7	356	303	0.458	0.441
829	66	68.81	127	122	193	190.8	359	353	0.538	0.541
830	67	55.57	98	103.5	165	159.1	370	353	0.446	0.451
831	60	56.05	91	100.7	151	156.8	388	382	0.389	0.41
832	45	27.45	135	130	180	157.5	427	397	0.422	0.397
833	52	49.48	93	91	145	140.5	323	298	0.449	0.471
834	45	40.61	82	76.24	127	116.8	318	290	0.399	0.403
835	50	45.31	95	90.91	145	136.2	372	351	0.39	0.388
836	56	42.22	109	107.9	165	150.1	365	360	0.452	0.417
838	50	40.96	78	75.5	128	116.5	305	285	0.42	0.409
839	52	45.73	95	95.22	147	140.9	322	303	0.457	0.465
840	56	44.77	106	105.9	162	150.7	323	317	0.502	0.475
841	57	50.35	84	83.34	141	133.7	333	306	0.423	0.437
842	43	35.04	100	99.59	143	134.6	348	349	0.411	0.386
843	50	39.47	103	115	153	154.5	365	355	0.419	0.435
844	60	43.8	92	96.64	152	140.4	376	374	0.404	0.375
845	28	20.91	133	134.4	161	155.3	339	339	0.475	0.458
846	61	54.64	104	123	165	177.6	351	351	0.47	0.506
847	57	50.11	111	141.4	168	191.5	371	371	0.453	0.516
848	63	39.46	102	99.72	165	139.2	392	389	0.421	0.358
850	51	57.92	87	102.3	138	160.3	387	389	0.357	0.412
851	61	52.01	68	79.89	129	131.9	324	322	0.398	0.41

IMG NO	RCD		LCD		CD		TD		CTR	
	R	P	R	P	R	P	R	P	R	P
852	72	60.09	90	110	162	170.1	351	346	0.462	0.492
853	49	37.09	84	85.24	133	122.3	362	363	0.367	0.337
854	33	23.02	97	96.84	130	119.9	345	341	0.377	0.352
855	51	37.59	83	80.6	134	118.2	315	276	0.425	0.428
856	61	51.07	102	107.9	163	158.9	334	331	0.488	0.48
857	45	34.08	111	101.3	156	135.3	379	373	0.412	0.363
858	49	39.7	119	116.7	168	156.4	378	379	0.444	0.413
859	50	40.43	117	131.3	167	171.7	399	395	0.419	0.435
860	60	50.97	110	128.5	170	179.5	367	365	0.463	0.492
861	66	50	87	81.98	153	132	402	405	0.381	0.326
863	39	27.79	103	103.7	142	131.5	332	330	0.428	0.399
864	56	49.61	75	77.68	131	127.3	325	319	0.403	0.399
865	49	42.04	73	74.6	122	116.6	306	295	0.399	0.395
866	53	37.51	99	98	152	135.5	333	331	0.456	0.409
867	43	33.63	89	87.85	132	121.5	320	304	0.413	0.4
868	46	41.97	83	79.33	129	121.3	321	320	0.402	0.379
869	50	32.96	104	102.2	154	135.1	362	355	0.425	0.381
870	35	26.7	104	91.52	139	118.2	340	307	0.409	0.385
871	40	31.28	93	97.36	133	128.6	328	323	0.405	0.398
872	36	21.64	91	102	127	123.6	324	327	0.392	0.378
873	57	42.35	80	79.27	137	121.6	333	325	0.411	0.374
874	50	37.83	68	70.95	118	108.8	283	287	0.417	0.379
876	49	36.99	124	125.8	173	162.8	361	331	0.479	0.492
877	42	24.59	126	131.7	168	156.3	329	326	0.511	0.479
878	45	39.69	113	117.2	158	156.9	367	367	0.431	0.427
879	55	46.76	117	95.56	172	142.3	367	367	0.469	0.388
880	51	38.55	91	93.41	142	132	344	343	0.413	0.385
881	46	28.2	108	102.8	154	131	383	377	0.402	0.348
882	60	47.01	79	83.35	139	130.4	347	350	0.401	0.372

IMG NO	RCD R	RCD P	LCD R	LCD P	CD R	CD P	TD R	TD P	CTR R	CTR P
883	65	49.13	91	93.83	156	143	358	359	0.436	0.398
884	60	48.02	107	111	167	159	367	375	0.455	0.424
885	41	28.88	123	120	164	148.9	338	329	0.485	0.453
886	70	49.38	92	106.4	162	155.7	376	374	0.431	0.416
887	46	44.13	138	141	184	185.1	407	398	0.452	0.465
888	68	59.1	107	123	175	182.1	376	377	0.465	0.483
889	43	35.54	112	117.7	155	153.3	351	352	0.442	0.435
890	36	27.84	110	110	146	137.8	356	358	0.41	0.385
892	37	29.63	135	122	172	151.6	400	381	0.43	0.398
893	60	47.4	83	94	143	141.4	317	293	0.451	0.483
894	54	37.86	116	114	170	151.9	367	364	0.463	0.417
895	53	43.23	100	101	153	144.2	318	314	0.481	0.459
896	58	50.08	100	104	158	154.1	321	317	0.492	0.486
897	50	49.31	86	89.14	136	138.5	326	324	0.417	0.427
898	43	32.91	91	94.99	134	127.9	374	374	0.358	0.342
899	41	29.35	120	114	161	143.4	342	335	0.471	0.428
900	50	43.6	102	106.3	152	149.9	386	376	0.394	0.399
901	44	30.53	97	102.4	141	132.9	340	341	0.415	0.39
902	55	38.43	100	101.6	155	140.1	358	359	0.433	0.39
903	56	45.34	73	80.9	129	126.2	309	307	0.417	0.411
904	52	46.42	84	83.99	136	130.4	305	275	0.446	0.474
906	41	27.92	101	99.6	142	127.5	298	299	0.477	0.427
907	43	31.8	117	121	160	152.8	324	301	0.494	0.508
908	41	30.56	124	131	165	161.6	380	369	0.434	0.438
909	58	48.15	107	112	165	160.1	377	379	0.438	0.423
910	65	35.07	82	93.02	147	128.1	349	346	0.421	0.37
911	56	45.99	117	123	173	169	364	367	0.475	0.46
913	42	34.91	113	111.4	155	146.3	358	347	0.433	0.422
914	56	42.11	99	99.89	155	142	332	314	0.467	0.452

IMG NO	RCD R	RCD P	LCD R	LCD P	CD R	CD P	TD R	TD P	CTR R	CTR P
915	43	31.59	100	102.2	143	133.8	346	348	0.413	0.385
916	55	46.8	102	104	157	150.8	343	340	0.458	0.444
917	51	33.49	106	104.4	157	137.9	383	381	0.41	0.362
919	48	57.2	98	93.02	146	150.2	369	361	0.396	0.416
920	69	48.19	98	115	167	163.2	358	351	0.466	0.465
921	50	36.44	114	116	164	152.5	357	358	0.459	0.426
922	62	53.07	131	149	193	202.1	396	378	0.487	0.535
923	56	52.77	108	115.7	164	168.5	391	375	0.419	0.449
924	43	33.12	106	105	149	138.1	337	335	0.442	0.412
925	32	27.8	128	126	160	153.8	385	378	0.416	0.407
926	71	55.23	116	119.7	187	174.9	392	386	0.477	0.453
927	52	45.12	112	120	164	165.1	386	378	0.425	0.437
928	58	52.96	106	108	164	161	351	351	0.467	0.459
929	62	44.33	104	103	166	147.3	383	378	0.433	0.39
930	49	39.82	111	109	160	148.9	337	333	0.475	0.447
931	63	44.57	113	115	176	159.6	355	353	0.496	0.452
932	52	42.95	109	120.8	161	163.8	343	341	0.469	0.48
933	36	22.8	113	137	149	159.8	369	370	0.404	0.432
934	25	14.77	116	115	141	129.8	345	341	0.409	0.381
935	46	40.21	111	109.1	157	149.3	397	379	0.395	0.394
936	62	46.17	107	111	169	157.2	360	359	0.469	0.438
937	22	17.81	113	111.6	135	129.4	376	374	0.359	0.346
938	51	40.61	91	86.89	142	127.5	368	366	0.386	0.348
939	66	54.52	70	80.94	136	135.5	322	323	0.422	0.419
940	46	35.45	111	113	157	148.4	325	301	0.483	0.493
941	41	29.67	96	97	137	126.7	320	307	0.428	0.413
942	59	48.79	94	95	153	143.8	351	344	0.436	0.418
943	54	40.91	82	84.79	136	125.7	344	343	0.395	0.366
944	47	35.39	94	101	141	136.4	334	340	0.422	0.401

IMG NO	RCD R	RCD P	LCD R	LCD P	CD R	CD P	TD R	TD P	CTR R	CTR P
945	44	35.71	91	94.61	135	130.3	349	335	0.387	0.389
946	29	21.77	98	98.76	127	120.5	329	323	0.386	0.373
947	51	43.48	99	101.7	150	145.2	375	368	0.4	0.394
948	70	63.97	126	132.6	196	196.6	375	373	0.523	0.527
949	80	66.87	99	110.5	179	177.4	376	381	0.476	0.466
950	48	35.19	113	112	161	147.2	386	377	0.417	0.39
951	30	31.28	93	87.85	123	119.1	314	297	0.392	0.401
952	41	30.88	120	116.3	161	147.2	406	407	0.397	0.362
953	60	49.38	78	76.97	138	126.4	355	347	0.389	0.364
954	63	53.53	118	130.8	181	184.3	401	387	0.451	0.476
955	51	34.92	109	107	160	141.9	356	348	0.449	0.408
956	42	38.63	117	118	159	156.6	373	361	0.426	0.434
957	54	51.98	125	130	179	182	375	372	0.477	0.489
958	70	67.1	146	148.1	216	215.2	427	416	0.506	0.517
960	50	41.8	112	111.5	162	153.3	381	370	0.425	0.414
961	59	48.87	96	96.35	155	145.2	401	404	0.387	0.359
962	65	60.75	115	111	180	171.7	404	385	0.446	0.446
963	65	56.01	125	127	190	183	375	364	0.507	0.503
964	46	36.95	135	139.4	181	176.4	378	352	0.479	0.501
965	47	37.12	101	102.9	148	140	355	357	0.417	0.392
967	46	32.56	109	112.6	155	145.2	357	359	0.434	0.404
968	62	45.16	91	92.13	153	137.3	377	370	0.406	0.371
969	48	37.08	126	111.2	174	148.2	383	363	0.454	0.408
970	39	33.19	102	110	141	143.2	362	352	0.39	0.407
971	108	84.73	49	60.92	157	145.7	359	357	0.437	0.408
972	58	51.88	120	117	178	168.9	391	384	0.455	0.44
973	48	35.97	121	134.4	169	170.4	367	354	0.46	0.481
974	45	42.58	128	132	173	174.6	347	346	0.499	0.505
975	66	51.11	132	126	198	177.1	386	376	0.513	0.471

IMG NO	RCD R	RCD P	LCD R	LCD P	CD R	CD P	TD R	TD P	CTR R	CTR P
976	45	38.76	132	125	177	163.8	407	410	0.435	0.399
977	27	23.48	102	104	129	127.4	367	370	0.351	0.344
978	53	33.39	119	120	172	153.4	396	389	0.434	0.394
979	58	51.97	127	112	185	164	361	353	0.512	0.465
980	62	52.29	92	97.06	154	149.4	344	345	0.448	0.433
981	49	28.64	101	100	150	128.6	366	364	0.41	0.353
982	49	40.87	99	99.9	148	140.8	376	374	0.394	0.376
983	38	49.58	100	117	138	166.6	351	342	0.393	0.487
984	48	40.14	116	116.4	164	156.5	408	408	0.402	0.384

VITA

Wasin Poncheewin is a master's degree student majoring in Computer Science and Information Technology at department of Mathematics and Computer Science, Faculty of Science, Chulalongkorn University. He graduated in bachelor's degree with majoring in Computer Science at the same place in the year 2011.